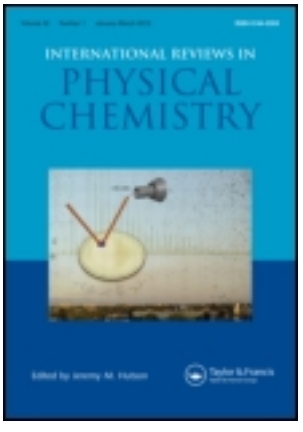

International Reviews in Physical Chemistry

Publication details, including instructions for authors and subscription information:
http://www.tandfonline.com/loi/trpc20

Excited state dynamics of DNA bases

Karl Kleinermanns [a] , Dana Nachtigallová [b] & Mattanjah S. de Vries [c]

[a] Institut für Physikalische Chemie und Elektrochemie, Heinrich Heine Universität Düsseldorf , 40225 , Düsseldorf , Germany

[b] The Institute of Organic Chemistry and Biochemistry , Flemingovo nám., 2, 166 10 Praha 6, Czech Republic

[c] Department of Chemistry and Biochemistry , University of California , Santa Barbara , CA , 93106-9510 , USA

Published online: 12 Mar 2013.

To cite this article: Karl Kleinermanns , Dana Nachtigallov & Mattanjah S. de Vries (2013) Excited state dynamics of DNA bases, International Reviews in Physical Chemistry, 32:2, 308-342, DOI: 10.1080/0144235X.2012.760884

To link to this article: http://dx.doi.org/10.1080/0144235X.2012.760884

International Reviews in Physical Chemistry, 2013
Vol. 32, No. 2, 308–342, http://dx.doi.org/10.1080/0144235X.2012.760884

Excited state dynamics of DNA bases

Karl Kleinermanns[a], Dana Nachtigallová[b] and Mattanjah S. de Vries[c]*

[a]*Institut für Physikalische Chemie und Elektrochemie, Heinrich Heine Universität, Düsseldorf 40225, Düsseldorf, Germany;* [b]*The Institute of Organic Chemistry and Biochemistry, Flemingovo nám., 2, 166 10 Praha 6, Czech Republic;* [c]*Department of Chemistry and Biochemistry, University of California, Santa Barbara, CA 93106-9510, USA*

(*Received 21 September 2012; final version received 18 December 2012*)

Biochemical reactions are subject to the particular environmental conditions of planet earth, including solar irradiation. How DNA responds to radiation is relevant to human health because radiation damage can affect genetic propagation and lead to cancer and is also important for our understanding of how life on earth developed. A reductionist approach to unravelling the detailed photochemistry seeks to establish intrinsic properties of individual DNA building blocks, followed by extrapolation to larger systems, to incorporate interactions between the building blocks and the role of the biomolecular environment. Advances in both experimental and computational techniques have lead to increasingly detailed insights in the excited state dynamics of DNA bases in isolation as well as the role of the solvent and intermolecular interactions. This review seeks to summarise current findings and understanding.

Keywords: DNA bases; nucleobases; excited state; lifetime; dynamics; UV; computations; gas phase; conical intersections

Contents

*Corresponding author. Email: devries@chem.ucsb.edu

1. Introduction

Understanding the response of DNA bases to UV radiation is critical for both practical and fundamental reasons: first, the nucleobase photochemistry following UV absorption constitutes a fundamental step in radiation-induced DNA damage. Second, UV photodynamics may have played a key role in prebiotic chemistry on an early earth. This is the chemistry that presumably took place four billion years ago and eventually produced the self-replicating molecules that form the basis of life as we know it today. Furthermore, studying nucleobase excited state dynamics provides detailed insights in electronic excited states and molecular structure, both of which are important in chemical interactions and reactivity. Finally, comparisons with the latest experimental data provide sensitive tests of *ab initio* theory of these fundamental processes.

A reductionist approach to the topic starts experimentally with isolated nucleobases in the gas phase, followed by nucleosides and nucleotides, inter base clusters and clusters with water and finally solution phase measurements. Along the way, the data on the one hand become less detailed while on the other hand incorporating more relevant parameters. The study of molecules isolated in the gas phase allows for observation of intrinsic properties and for optimal comparison with the highest levels of quantum computational theory. This first step is now leading to an increasingly detailed understanding of excited state dynamics at the molecular level. However, the resulting insights are still incomplete and need to be extrapolated to conditions that include the role of the environment. In fact, studies in solution or involving the macromolecule show that other structural elements also influence the excited state dynamics. For example, in the macromolecule base stacking competes with hydrogen bonding, or in an aqueous environment hydrogen bonding with water affects the excited state potentials and alters the excited state dynamics.

The current picture that emerges shows that for these compounds excited state dynamics depends very sensitively on molecular structure. Nucleobases are forms of purines and pyrimidines and the excited state lifetimes of these types of compounds can vary widely in a range from femtoseconds to nanoseconds. These remarkably large lifetime differences arise from small and subtle variations in molecular structure between similar derivatives, tautomers or cluster structures. This experimental observation has helped motivate a growing number of

theoretical studies that model the excited state dynamics with potential surfaces which include conical intersections (CI), mediating rapid internal conversion [1–11].

The time dependent properties of DNA in the gas phase and in solution have been the topic of recent reviews [12–14]. This review aims to summarise our current understanding of DNA excited state dynamics at the different levels of increasing complexity, starting from isolated molecules and extrapolating to more complete biological environments.

2. Background

Molecular photostability is the complex outcome of intramolecular and intermolecular factors: one molecule can be intrinsically more resistant to light-induced damage than another even though they absorb UV light equally. The key photochemical events take place after a molecule absorbs a photon and reaches an excited electronic state. The resulting electronic excitation can initiate inter- or intramolecular chemical reactions. The electronic energy can be radiated away by fluorescence, but this process occurs typically with a rate constant of $\sim 10^9$ s^{-1} which is generally too slow to compete with an excited state reaction. Alternatively, the electronic energy can be converted to heat by internal conversion to the ground state; heat can subsequently be safely dissipated to the environment. When internal conversion is fast enough to prevent photochemical reactions from taking place, the molecule will have a very short excited state lifetime, τ, and be stable against UV photodamage [15].

Rapid internal conversion, when available to a molecule, provides a 'self-healing process' following the absorption of a photon: it dissipates electronic energy by converting it to internal energy in the ground state and therefore minimises access to other photochemical pathways. Generally the biologically most relevant forms of the purines and pyrimidines exhibit the shortest excited state lifetimes, thus selectively minimising the chances for photochemical damage in the molecular building blocks of life. In stark contrast, many other nucleobase derivatives, even isomers, have orders of magnitude longer lifetimes (See Figure 1). In fact, ultrafast internal conversion – the same property found in many UV sunscreens – is observed for all nucleobases implicated in replication today and, intriguingly, there are no examples of canonical nucleobases that are highly fluorescent [12]. Illustrating the correlation between excited state lifetime and the propensity for photoreaction is the observation that the minor DNA base 5-methylcytosine, with its 10-fold longer lifetime than cytosine, is a hot spot for photodamage [17].

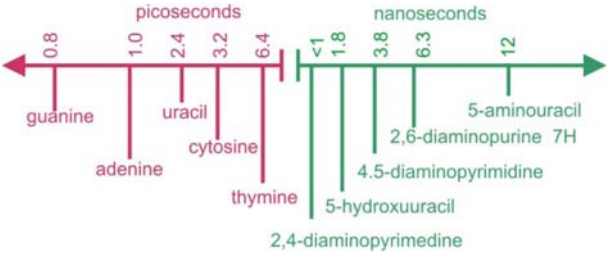

Figure 1. (Colour online) Compilation of gas phase excited state lifetimes of selected nucleobases and derivatives. For a study of substitution effects on the photochemical properties of aminopyrimidines see [16].

Evolution requires the existence of self-replicating molecules; the selection of the nucleobases as building blocks of those macromolecules would thus logically have taken place prior to any biological processes. Therefore, if the excited state properties have played a role in a chemical selection of today's nucleobases, they may be a relic of prebiotic chemistry on an early earth. These photochemical properties then would be molecular fossils, so to speak, of four-billion-year-old chemistry.

Self-protection by internal conversion depends dramatically on molecular structure. The intramolecular mechanism governing the ultrafast internal conversion in these compounds is now emerging. The key is the occurrence of CI that connect the excited state potential energy surface (PES), reached by photon absorption, to the ground state energy surface. The dramatic lifetime differences between derivatives of nucleobases appear to be due to variations in the excited state potential surfaces that restrict or slow access to these CI [18].

We can rationalise these differences as illustrated schematically in Figure 2. CI are the crossings of multidimensional potential surfaces. Therefore these features can only occur in regions of the potential energy landscape that represent a deformation of the molecular frame from the ground state equilibrium geometry. The following case study of adenine derivatives serves as an example [4,13,19–30]. For 4-aminopyrimidine (Figure 3 bottom left), surface hopping calculations identified two main CI [31]: deformation at the C2 position leads to deactivation of the excited state with a lifetime, τ, of 1 ps and deformation at the C5=C6 bond leads to different dynamics. Immobilising the latter coordinate with a five-membered ring forms adenine with a conical intersection due to the C2 deformation and τ of 1 ps. Figure 3 shows the geometry at this conical intersection as calculated by Marian *et al*. [4]. Substitution at the C2 position further modifies the excited state potential and eliminates this conical intersection. Consequently, both 2,6-diaminopurine and 2-aminopurine have fluorescent excited states with lifetimes of the order of nanoseconds. In fact, the latter is used as a fluorescent tag in DNA research. For 2,6-diaminopurine, Gengeliczki *et al*. measured tautomer-dependent excited state lifetimes of 6.3 and 8.7 ns for the 9H– and 7H-diamino forms, respectively [32]. Other excited states also need to be considered: N9-H motion forms an additional coordinate

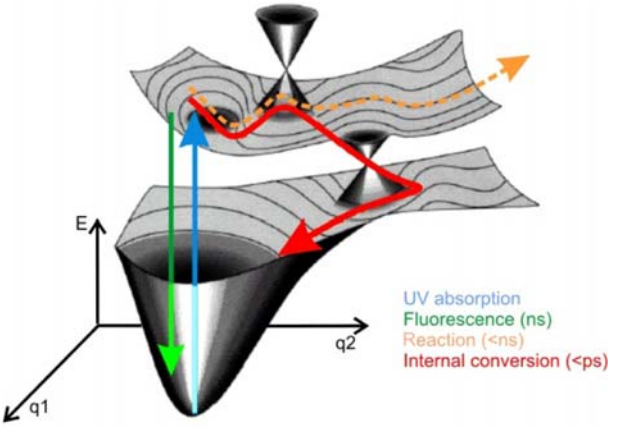

Figure 2. (Colour online) Schematic 3D potential energy diagram with two CI connecting the S_1 excited state with the S_0 ground state. The q1 and q2 are molecular coordinates.

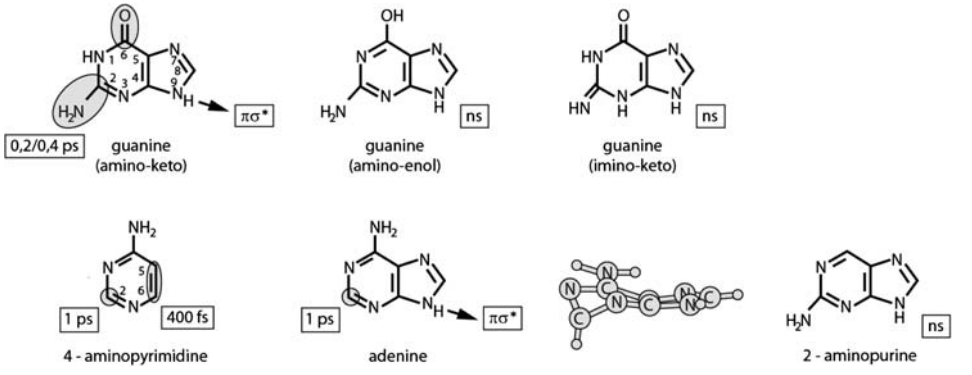

Figure 3. C2 ring deformation with the NH_2 group distorted from the plane and to a minor extent out-of-plane C=O deformation lead to CI and ultrafast internal conversion in amino-keto guanine. The imino and enol tautomers have several orders of magnitude longer lifetimes. Ring deformations at C2 or C5=C6 in adenine lead to CI that mediate internal conversion at different timescales depending on molecular structure. Details in text below.

in adenine that can lead to a conical intersection with a $\pi\sigma^*$ state [29,33]. This coordinate forms a more general internal conversion motif that possibly also plays a role in peptides [34]. A weakly absorbing $n\pi^*$ state plays a role as well, in addition to the $\pi\pi^*$ state, and can sometimes serve as a 'dark state' with an extended lifetime [35,36].

Furthermore, purine, the parent compound of adenine as well as guanine, forms triplet states in high yield [37]. Lifetimes also depend strongly on tautomeric forms and on substitution [11,13,38–40]. For example, the biologically relevant keto form of guanine is short lived, in stark contrast to the very long-lived enol and imino forms [3,35,41–49] (see Fig. 3 top). Understanding these mechanisms helps explain how subtle structural differences between substituted nucleobases can produce excited state lifetime differences of orders of magnitude.

In the same way, C5 substituents in pyrimidines alter excited state lifetimes over a range of picoseconds to nanoseconds, by modification of the topography of the PESs around C5=C6 torsion and stretching coordinates [2,50,51]. Interestingly, the same coordinates are found to play a role in thymine photo-dimerisation in DNA [52]. Figure 4 summarises the findings of Nachtigallová *et al*. for five-substituted uracil [5]. Both canonical bases uracil and thymine, which is 5-methyluracil, exhibit broad UV spectra in the gas phase indicative of short excited state lifetimes, while substitution with OH or NH_2 leads to lifetimes of 2 and 12 ns, respectively. This observation underscores the point that the role of the substituent is not merely to block an out-of-plane deformation of the heteroatomic ring, but rather it modifies the excited state potentential energy landscape [53]. Calculations by Matsika and Kistler predict similar effects for substituted cytosine analogues [51,54].

2.1. *The effect of the environment*

As complexity increases, for example through base pairing or through the oligomerisation of mononucleotides, the mechanisms for safely eliminating excess electronic energy from biomolecules may change in dramatic ways. In a biological environment, molecules are embedded in a complex structure with multiple electrostatic interactions, hydrogen bonds and

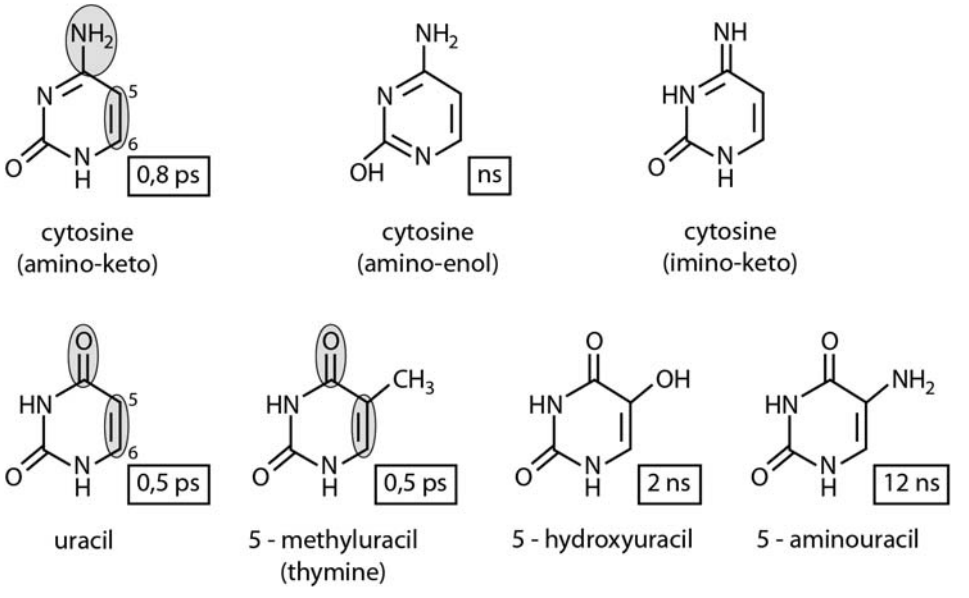

Figure 4. Twisting of the C5–C6 bond and out-of-plane NH_2 distortion lead to CI and ultrafast internal conversion in amino-keto cytosine upon excitation at 250 nm [56]. The vibronic spectrum detected by R2PI consists of just a few lines around 313 nm [57,58]. The amino-enol tautomer has a much longer lifetime with an extended electronic spectrum. The imino-keto tautomer was detected by microwave spectroscopy [59] but not yet by electronic spectroscopy. Twisting of the C5–C6 bond and out-of-plane distortion of the C=O group lead to CI and fast internal conversion in uracil and thymine whereas five-substituted uracils exhibit nanosecond lifetimes. The R2PI spectra of uracil and thymine are broad as expected from the short excited state lifetimes. Uracil and thymine also exhibit longer lifetime components of a few ps, see Section 4.3.

dispersion interactions such as stacking of the base π-systems [55]. The energy of electronically excited states, especially those with large dipole moments and facile polarisability of the electron density distribution, often sensitively depends on the interaction with this surrounding. The shape of the potential surface of the excited state, its energy gradients, the depths of its potential minima and the barriers for crossing from one minimum to another and finally to the singlet or triplet ground state is modulated by the surrounding molecules. Furthermore, the solvent molecules or subgroups of interacting macromolecules need time to relax to the new electron distribution, attained after optical excitation, which often changes the dynamics of the excited state significantly. New potential energy minima may develop upon relaxation of the surrounding of the excited chromophore, energy gradients change and barriers are modified

2.2. *The role of the solvent*

The role of the solvent is complex, because it not only affects excited state dynamics by hydrogen bonding interactions and structural changes, but also plays a role in subsequent quenching of internal excitation.

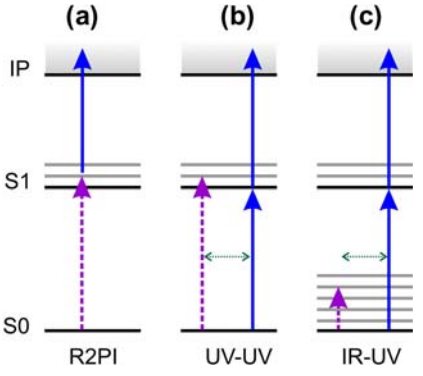

Figure 5. (Colour online) Schematic diagram of spectroscopic techniques. Dashed arrow indicates wavelength that is being scanned to obtain a spectrum. Solid arrows indicate fixed wavelength. Dotted horizontal arrows indicate time delay between two laser pulses. (a) R2PI provides vibronic spectra. (b) UV–UV hole burning separates isomeric contributions to the UV spectrum. (c) IR–UV hole burning provides isomer selected ground state IR spectra. In (b) and (c), the ion signal from the fixed wavelength second laser pulse (probe) decreases at each wavelength of the first pulse (burn) that is resonant and thus depletes the ground state in the FC region.

In nonradiative decay, the absorbed photon is converted into excess vibrational energy such that the vibrational temperature of a nucleobase exceeds 1000 K immediately after internal conversion to the electronic ground state [60]. The ability of these hot ground state molecules to undergo thermal chemistry is unknown. Importantly, a hot ground state intermediate has been proposed for the photohydration reaction seen in uracil [61]. Fortunately, solvation allows this excess energy to be rapidly diluted by vibrational energy transfer outward first to nearest-neighbour solvent molecules, and then to the next-nearest neighbours. Thus, internal conversion is followed by extremely rapid diffusion of heat until the excess vibrational energy has been completely thermalised. This energy transferred to the environment makes rapid internal conversion an effective protection mechanism, neutralising otherwise potentially harmful UV absorption. Interestingly, water, the solvent of life, gives rise to the fastest rate of intermolecular energy transfer, permitting a hot ground state molecule to cool within just a few picoseconds – the highest rate of cooling observed in any solvent studied to date [62,63]. For single bases in aqueous solution, the key appears to be hydrogen bonds between neighbouring water molecules and with nucleobases leading to low frequency intermolecular vibrations and a corresponding high vibrational state density as required for efficient energy transfer. In a duplex, hydrogen bonds between strands could play a similar role in safely dispersing excess vibrational energy. For an isolated molecule, where such intermolecular vibrational energy transfer is impossible, photofragmentation eventually occurs but not on the limited time scale of most gas phase experiments.

In Section 3, we will summarise the main methods employed in these studies. Then we will detail information on each of the canonical bases, experimentally and computationally in Section 4. We will cover interactions between bases and their environment, such as pairing, stacking and hydrogen bonding with solvents in Section 5.

3. Methods

Spectroscopy in the gas phase requires a way to vaporise and subsequently cool the molecules. For neutral species, the combination of laser desorption and jet cooling has been successful, achieving internal temperatures of the order of 20 K, usually sufficient for reducing vibrational populations to $v = 0$ [64,65]. For ions, electrospray ionisation can be combined with cooling in an ion trap, achieving even lower temperatures, approaching that of liquid helium, and thus enabling even higher spectral resolution and extending the size range of molecules that can be analysed [66]. For neutrals, electronic spectroscopy usually is action spectroscopy in the form of resonant two-photon ionisation (R2PI) or laser-induced fluorescence (LIF). The former has the advantage of mass selection while the latter may be augmented by dispersion of the fluorescence. In either case, when employing nanosecond excitation pulses, the technique is essentially blind for excited states with lifetimes in the sub-picosecond range while line widths may be used to estimate lifetimes in the sub-nanosecond range. Double resonant spectroscopy combines these forms of electronic spectroscopy with UV or IR hole burning. A burn laser pulse precedes the R2PI or LIF probe pulse such that on resonance it removes ground state population from the Franck–Condon (FC) region and thus reduces the probe laser signal, resulting in an ion-dip or fluorescence-dip spectrum. With an IR burn laser this technique essentially produces a ground state IR spectrum with optical selection by the probe laser and, in the case of R2PI, also additional mass selection. This powerful approach makes it possible to obtain isomer specific data, with a selectivity unmatched by condensed phase techniques. For ions, spectroscopy can often be performed by various forms of infrared multiphoton dissociation. In that case, the isomer specificity is lost but mass selection is an integral part of all ion spectroscopy techniques.

Femtosecond pump–probe experiments are possible in the gas phase but very challenging, due to the inherent low density of the sample. Such experiments are therefore more often performed in the condensed phase and various techniques have been developed, such as transient absorption and fluorescence up-conversion. Simple electronic absorption and emission spectra of complex molecules in the condensed phase are often quite broad with little apparent structure and therefore rather unspecific for excited state dynamics. If, however, absoption or emission are followed from the femtosecond to the nanosecond time scale a new dimension is added and spectral changes can intimately reflect the fate of the excited state time step by time step. Early in the dynamics, relaxation proceeds within a few tens of femtoseconds from higher electronically excited states to lower ones followed by fast motions along steep energy gradients on the lower excited surface. With sufficient time and (broadband) spectral resolution this dynamics can be followed without interference from events at later times. At later times, but often still in the sub-picosecond range, motion of the molecular wave packet (WP) follows along flat parts of the potential surface and from one minimum to another through small barriers. Still later internal conversion to the electronic ground state or intersystem crossing to the triplet state occurs followed by vibrational cooling within a few picoseconds (in H-bonded systems). Femtosecond pump–probe absorption spectroscopy can elucidate conversion between different dark and bright states and between chemical species, based on multiexponential decay times. Broad-band transient absorption spectroscopy is particularly informative because rather than monitoring kinetics at selected wavelengths it gives the complete spectral evolution in a broad range, typically 270–1000 nm. This technique sheds light on the dynamics of both bright and dark states and allows

discrimination between spectral shifts (due to e.g. vibrational cooling or solvent relaxation) from conversion processes between different electronic states and chemical species. If furthermore excitation is performed at different wavelengths (that is at different vibrational excess energies in the electronically excited state) and at different polarisation angles between pump and probe laser, a detailed picture emerges of excited state dynamics. Variation of the sample conditions like pH and temperature can complement such studies. Femtosecond fluorescence up-conversion spectroscopy is another valuable method which selectively monitors the fate of the bright excited states. This selectivity often facilitates interpretation of the complex transient spectra but no information about the (dynamically often important) dark states can be obtained. With this method it may be difficult or even impossible to discriminate between fast relaxation to the ground state or to a dark lower excited state. On the other hand comparison of fluorescence up-conversion and transient UV/Vis and IR absorption results may help to discriminate between dark and bright state transitions in the absorption spectra [67].

3.1. *Clusters*

Gas phase clusters with water and other solvent molecules with varying H-bonding capability, polarity and dielectric constant make it possible to study the shift of electronic states and change of dynamics step by step, progressing from small to large clusters. This approach can reveal details of microsolvation, by observing the effects of successively adding one single solvent molecule at a time. Examples are the well-known red shift of $\pi\pi^*$-transitions and blue shift of $n\pi^*$-transitions in many chromophores undergoing H-bonding. The $\pi\pi^*$-excited state is more acidic and therefore more stabilised than the ground state due to a stronger H-bond (red shift of the optical transition) while H-bonding is weakened by transferring an electron from a nonbinding orbital at the heteroatom involved in the H-bond to a π^*-orbital (blue shift). Even more dramatic is the shift of the energy of a charge transfer (CT) state with ultrahigh dipole moment in a polar surrounding compared to an non-polar state or to isolation in the gas phase. There is however a size limitation of meaningful cluster investigations via high-resolution spectroscopy. The number of isomers increases and the spectra get more and more congested and complex due to underlying complex dynamics, high state density and insufficient cooling. The jets warm up due to the energy released by formation of large aggregates. Under those conditions it can become difficult to sufficiently cool the molecular beam even in an expansion with heavy inert gases like xenon [68]. Heavy and polarisable inert gases can improve cooling but are often problematic due to their extensive clustering. If REMPI is used for analysis, cluster fragmentation may complicate size assignment because large clusters frequently tend to fragment already at the adiabatic ionisation threshold. Even sophisticated double- and triple-resonance laser spectroscopic techniques reach their limit of reliable analysis above certain cluster sizes.

Significant changes of the energies of the excited state and modifications of the energy surface may well occur at larger cluster sizes than experimentally accessible. An incomplete first solvation shell may reflect the relevant potential energy modifications of the isolated chromophore in the excited state sufficiently accurate; however, it can be experimentally impossible to reliably analyse clusters of this size. If so, it is necessary to change to the condensed phase and investigate the biomolecular building blocks either in defined films or in the liquid phase for comparison with the gas phase.

3.2. *Computational state-of-the-art*

Computational studies performed on excited states of isolated nucleic acid bases, especially in the last 10 years, shed light on relaxation mechanisms that are not directly accessible experimentally [69]. A general strategy for investigation of excited state dynamics involves calculation of spectra in the FC region of the ground state minimum, followed by determination of critical points on the excited state potential surfaces, particularly excited state minima and structures at the crossing of adiabatic PESs [69,70]. These crossings, known as CI, provide pathways for fast radiationless relaxation of a molecule to the ground state. The efficiency of this process depends on the relative energies of critical points and the details of reaction trajectories on the potential surfaces connecting them. To obtain a balanced description of these characteristics the choice of a suitable computational method is crucial.

For *ab initio* descriptions, single-reference methods are reliable for calculations of excitation energies in the region of ground state minima. The approximate coupled-cluster singles-and-doubles model (CC2) [71] and the second-order algebraic diagrammatic construction (ADC2) [72,73] with resolution-of-the identity [74] provide good and efficient methods for calculating vertical excitation spectra. These methods can also be used to calculate analytical gradients to find excited state minima [75]. Density functional theory (DFT) methods are an alternative choice for calculating excited state energies, especially for systems of moderate size. The linear response time-dependent (TD) approximation is one of several such approaches [76]. For these methods, the energy gradients and nonadiabatic coupling vectors are also available [77–82].

Outside the FC region single-reference descriptions often fail due to the multi-reference character of the wavefunction. In such cases, the multi-configurational self-consistent field (MCSCF) method [83] may be used to obtain a correct wavefunction. Multi-configurational descriptions are particularly important near CI at the energy degeneracy between electronic states. Yet such methods still do not necessarily guarantee sufficiently accurate results of excited state energies. The reason is an insufficient description of electron correlation effects which might result in a different ordering of states. Thus, results obtained with the MCSCF method should always be checked with more advanced methods, e.g. multi-reference configuration interaction (MRCI) [84,85], or the complete active space perturbation theory to the second order (CASPT2) [86] methods. Analytical gradients [87–89] and nonadiabatic coupling terms [90], necessary to locate excited state minima and CI, are available in the multi-reference description. An alternative approach for describing the PESs of excited states of nucleobases is the use of semi-empirical methods, in particular the recently implemented configuration interaction method OM2/MRCI [91].

In principle, conventional quantum chemical calculations can provide useful information about the excited state behaviour of nucleobases. These approaches are based on knowledge of the PES, with emphasis on the energies of critical points and the reaction paths connecting them. They are, however, not sufficient to explain the relaxation dynamics of nucleobases when more relaxation channels are expected to be involved. To obtain a more complete description, simulation studies of the dynamics should be performed. Such studies have been undertaken for all five nucleobases at the *ab initio* [92–95], semiempirical [96–100] and density functional [101,102] levels. From these results, one can see that the interpretation of the experimentally observed features depends on the computational level used for dynamics simulations. To explain differences in excited state behaviour among nucleobases, it is

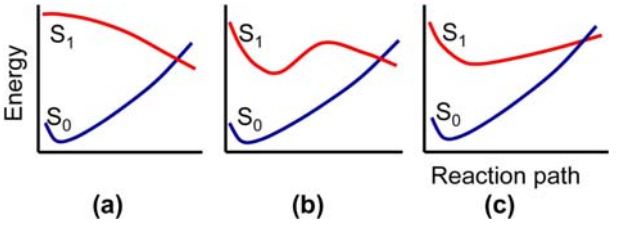

Figure 6. (Colour online) Relaxation paths connecting stationary points and conical intersection showing (a) descending character, (b) a barrier on the S_1 surface and (c) ascending character. An ultrafast relaxation corresponds to the character of S_1 shown in (a). The character of the S_1 surfaces (b) and (c) slow down the relaxation process. Figure adapted from [103].

important to use data which are obtained with comparable accuracy. Barbatti *et al*. performed studies at very similar levels of theory, based on the multi-configurational description of wavefunctions, for all five nucleobases [95]. This led to the explanation of variations in the relaxation mechanisms among the purine bases adenine and guanine and the pyrimidine bases thymine, uracil and cytosine (Figure 5).

CI play a key role in the nonadiabatic relaxation mechanism, however not all CI are effective in dynamics simulations. Knowledge about the relative energies of these structures with respect to energies of excited states at the ground state geometry and at the excited state minima, together with the character of reaction paths connecting them, can provide detailed insights into the relaxation mechanism. Among the reaction paths illustrated in Figure 6, a downhill motion from the initial point (either from the vertical FC region or from the minimum of the excited state) towards a particular structure on the crossing seam (panel a) makes this conical intersection quite efficient. Presence of a barrier (panel b) or an ascending character (panel c) of the reaction path slows down the relaxation process.

In the following section, we will discuss the results of 'static' and 'dynamic' interpretations of the relaxation mechanisms for each of the individual nucleobases separately, with emphasis on the differences between purine- and pyrimidine-based nucleobases. We will also discuss the remarkable difference between the excited state behaviour of thymine and uracil, which are quite similar structures.

4. The canonical bases – experiment and theory

4.1. *Guanine*

The ultrashort excited state lifetime of the canonical keto-amino tautomer of guanine prevented the measurement of its electronic spectrum in the gas phase via REMPI. Only the spectra of the nonnatural enol-amino and keto-imino tautomers of guanine could be obtained by IR–UV spectroscopy [41,104–107]. This case illustrates a number of aspects of these studies. Initial confusion of the spectral assignments resulted from the fact that the keto forms were predicted by theory to be lowest in energy, while their IR spectra are very similar to those of the imino forms. This similarity points to the need of high-resolution computations for proper interpretation of experiments. The fact that the keto tautomers were not observed could either mean that they do not exist in the gas phase experiment or that they are merely not detected. The latter possibility underscores the fact that action spectroscopy is blind for species with excited states that have lifetimes significantly shorter than the laser pulse. In fact,

the keto tautomer frequencies were eventually observed in helium droplets [43]. Those are in fact infrared absorption experiments that do not involve the electronically excited state. The results do reflect gas phase populations because the molecules are entrained into the droplets from the gas phase. Therefore this result clearly suggests that indeed the keto form exists in the gas phase but may go undetected in R2PI experiments because of a short lived excited state, in contrast to the other tautomeric forms.

Femtosecond spectroscopy of the nucleobase guanine provides an instructive example of the power of complimentary studies in the gas phase and in aqueous solution. Canuel *et al*. report biexponential decay with $\tau_1 = 0.15$ ps and $\tau_2 = 0.36$ ps for jet-cooled guanine excited at 267 nm and analysed via two-photon ionisation at 400 nm [35]. They interpreted τ_1 as WP motion from the FC region of the lowest excited $\pi\pi^*$ state L_a to its local minimum $L_{a\ min}$ and τ_2 by $L_{a\ min}/n\pi^*$ and $n\pi^*/S_0$ barrier crossings. Based on their computational studies Chen *et al*. [108] ascribed τ_2 to direct $L_{a\ min}/S_0$ barrier crossing without involvement of the $n\pi^*$ state. Serrano-Andres *et al*. did not detect any $L_{a\ min}$ in their calculations and ascribed τ_1 to arise from a barrierless motion on L_a toward the L_a/S_0 conical intersection (CI).

How does the same system behave in water? Kovalenko *et al*. used femtosecond broadband absorption spectroscopy to study the dynamics of guanosine monophosphate (GMP) in aqueous solutions [107] and compared the dynamics of the observed transients to quantum-chemical calculations by Improta. In the pH range of 7–4, GMP is nonprotonated at the guanine ring and shows biexponential decay in the probe region of 400–900 nm. With $\tau_1 = 0.22$ ps and $\tau_2 = 0.9$ ps, the relaxation is somewhat slower than in the gas phase and probably controlled by solvent rearrangement in the excited state. Between 270 and 400 nm, the signal response is triexponential with one growing ($\tau_1 = 0.25$ ps) and two decaying components ($\tau_2 = 1.0$ ps, $\tau_3 = 2.5$ ps). In this spectral range, guanine fluoresces and stimulated emission (SE) contributes to the absorption signal. The initial signal increases due to the decaying contribution from SE (observed as negative absorption). Transient anisotropy can elegantly discriminate between excited state absorption and SE, because the two signal contributions respond very differently to laser polarisation [107].

Broadband transient absorption directly monitors the motion of the WP on the excited state PES: τ_1 corresponds to motion away from the FC region to flatter parts of the surface where the WP resides for a moment and fluoresces (with SE) at ~320 nm, τ_2 represents internal conversion from L_a to S_0, and τ_3 corresponds to vibrational cooling of hot ground state molecules. The latter is only observable at less than 400 nm and to the red of the $S_0 \rightarrow L_a$ absorption. SE at ~400 nm points to another flat region on the L_a surface where GMP fluoresces before internal conversion takes place [107].

Fluorescence spectroscopy directly monitors the decreasing energy gap between S_1 and the ground state along the path to the conical intersection with the S_0 state. Fluorescence decay times of 2–4 ps at > 450 nm indicate that part of the wavepacket explores further flat or minimum regions of the excited state surface before conversion to the ground state [109]. The behaviour in both the transient absorption and fluorescence up-conversion experiments is independent of the excitation wavelength indicating ultrafast ($\ll$100 fs) $L_b \rightarrow L_a$ conversion.

At pH 2, the guanine ring is protonated at the N7 position [110]. The excited state dynamics of $GMPH^+$ is slower: a growing component with $\tau_1 = 0.4$ ps followed by a $\tau_2 = 2.3$ ps decay and internal conversion at $\tau_3 = 167$ ps indicate deeper potential minima and a larger barrier at the conical intersection to the S_0 state than for neutral GMP, see Figure 7. SE occurs at early times at 320 nm and later at 400 nm, similar to GMP however the corresponding fluorescence

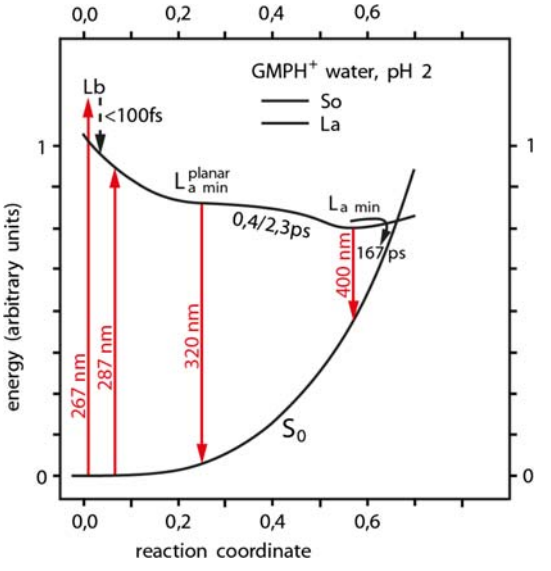

Figure 7. (Colour online) Schematic potentials of the excited state L_a and ground state S_0 surfaces of $GMPH^+$. At 267 nm excitation, both the L_a and L_b states are populated nearly equally while at 287 nm only the L_a state is excited. The observed dynamics are the same indicating ultrafast ($\ll$100 fs) $L_b \rightarrow L_a$ conversion. The $L_{a\ planar} \rightarrow L_{a\ min}$ transition occurs through a small barrier, with $\tau_1 = 0.4$ ps and $\tau_2 = 2.3$ ps. $L_{a\ min}$ is a well-defined minimum with NH and CH groups displaced out of the guanine ring and gives rise to strong fluorescence at 400 nm. Fluorescence and transient absorption decay with 167 ps, indicating a substantial barrier for conversion to the electronic ground state. Potential surface features and wavepacket evolution of GMP are qualitatively similar, however, potential minima are much flatter and evolution is nearly barrierless leading to ultrafast excited state kinetics and very weak fluorescence. For details, see text. Figure is adapted from [107].

of $GMPH^+$ is much stronger due to the slower kinetics on the excited state surface. Time-dependent density functional theory (TDDFT) calculations using the PBEO functional with explicit calculation of the first water solvation shell and bulk solvent effects accounted for by the polarisable continuum model reflect the energy scheme in Figure 7 very well. According to the calculations, the stable minimum $L_{a\ min}$ of $GMPH^+$ is characterised by out-of-plane displacement of NH and CH groups which explains the slower internal conversion and longer (167 ps) fluorescence lifetime [110,111]. The calculations show that the L_a and L_b excited states are involved in the excited state dynamics of GMP and $GMPH^+$ whereas the dark $^1n\pi^*$ and $\pi\sigma^*$ states have too high energies to play a significant role.

The UV-induced vibrational dynamics of GMP was studied by femtosecond infrared spectroscopy [112]. Rapid IC to a hot ground state was observed without excitation of the phosphate vibrations. Vibrational cooling with repopulation of the guanine ring vibrational ground state takes place within 2–4 ps in water in good agreement with Karunakaran *et al.* [107].

Femtosecond measurements of nucleobase excited state decays, determination of lifetimes from spectral bandwidths, or the existence or absence of R2PI spectra reveal rates of ultrafast internal conversion via CI. However, the molecular structures at the CIs remain obscure. Qualitative information about these structures can be obtained by a systematic study of derivatives of the nucleobases and tautomers where out-of-plane deformations of the ring system

are blocked and the excited state surface is modified, see Figures 3 and 4 and discussion above. For a quantitative comparison, however, dynamics calculations based on realistic excited state PESs are needed together with results from femtosecond measurements.

Among the five naturally occurring nucleobases, 9H-keto-guanine exhibits the shortest excited state lifetime in the gas phase, see Figure 3. Three types of CI have been identified on the S_1/S_0 crossing seam. Two of them, labelled as *ethylenic I* and *ethylenic II* [3,9,95,96,108,113,114], feature structures with a strongly puckered pyrimidine ring, with the largest puckering at the C2 atom and with the NH_2 group distorted from the plane. The wavefunctions of these CI result from mixing of $\pi\pi^*$ and closed shell electronic configurations. These two CI differ only by the orientation of the amino groups with respect to the six-membered ring. In the third type of conformation, the wavefunction is characterised by a mixing of the $n\pi^*$, $\pi(O)\pi^*$ and closed electronic configurations. In this structure (labelled as *oop*-O), the pyrimidine ring is puckered at the C6 atom with the oxygen atom distorted from the plane of the ring [3,9,96,114]. An S_1 minimum which is of $n\pi^*$ character was localised in the same energy region as the CI introduced above [9,108]. The calculated character of the PES suggests two possible relaxation mechanisms according to which (i) the molecule relaxes directly to the ethylenic conical intersection using a reaction path of $\pi\pi^*$ character or (ii) it first relaxes to the S_1 minimum with $n\pi^*$ character. These direct and indirect mechanisms provide an interpretation of experimentally observed relaxation times of 0.148 and 0.360 ps, respectively [9]. An alternative suggested relaxation pathway proceeds via a conical intersection with stretched NH bonds [115].

Dynamics simulation studies performed at the MR-CIS level resolve the relaxation mechanism and match the experimental data [114]. The initial conditions for these dynamics simulations were selected such that the system was excited into the bright state of $\pi\pi^*$ character. At the ground state minimum geometry, the $\pi\pi^*$ character corresponds to the S_1 state but it is almost isoenergetic with the S_2 state of $n\pi^*$ character allowing a reverse ordering of states within the coordinate space around the FC region. Thus, the trajectories are initially spread between the S_1 and S_2 states. In the latter case, there is an almost instantaneous $S_2 \rightarrow S_1$ relaxation on the time scale of about 20 fs [114]. The subsequent relaxation into the ground state involves a quite homogeneous mechanism. The vast majority of the population (95%) follows the direct $\pi\pi^*$ pathway towards the *ethylenic* CI. The rest of the population decays into the ground state via the *oop*-O conical intersection. The $\pi\pi^*$ relaxation mechanism was suggested also by a semi-empirical OM2 method [96]. The data obtained with the dynamics simulations study predict that guanine relaxes to the ground state with a single time decay constant of 0.22 ps, in very good agreement with experimentally estimated decay constants of 0.15 and 0.36 ps.

In guanosines, the biologically most relevant keto tautomer was not observed in gas phase REMPI experiments at the nanosecond timescale [116–118]. The assumption has been that this state is short lived. In another possible mechanism for nucleosides, the sugar moiety with its many degrees of freedom provides rapid quenching of vibronic energy in the excited state, thus bringing the system below the barrier and preventing or delaying internal conversion. Hare *et al*. have reported lifetimes in solution for the $n\pi^*$ state in pyrimidine nucleosides significantly longer than for free bases [46].

4.2. *Adenine*

The R2PI and double resonance spectra of jet-cooled adenine near 277 nm have been investigated by several groups [21,26,27,119,120]. The electronic spectrum consists of a few rather weak, but sharp peaks followed by a very broad band with onset around 275 nm. The observed vibronic structure has been assigned either to transitions to the lowest $\pi\pi^*$ (usually called L_a) state or to the $n\pi^*$ state or mixtures thereof whereas the broad band probably arises from transition to the next $\pi\pi^*$ (L_b) state with some possible contributions of higher $n\pi^*$ states. Transitions to the dissociative $\pi\sigma^*$ state probably play no role in the near UV spectral region at >250 nm [121,122], see, however, reference [123] for an alternative model.

Rotational contour resolved R2PI allows an unambiguous assignment of the vibronic bands around 277 nm because the transition moments of the $\pi\pi^*$ state should be predominantly in-plane with hybrid character of a and b rotational axes and some *c*-axis contribution in case of nonplanar distortion of the excited state. The $n\pi^*$ state, on the other hand, should show dominant c-type character. Indeed, the main vibronic bands of adenine could be assigned by this method [36]. The results show $\pi\pi^*$ and $n\pi^*$ transitions are within $< 50\,cm^{-1}$ of each other and close to 277 nm. They exhibit vibronic coupling by out-of-plane modes at higher energies where the transition moments of the $\pi\pi^*$ states are essentially in plane. Due to some nonplanarity in the excited states, the $^1n\pi^*$ state can borrow its intensity directly from the $^1\pi\pi^*$ state, explaining its unusual high intensity at low energies where vibronic coupling does not yet take place. The Lorentzian contribution to the width of the rotational contour points to excited state lifetimes > 10 ps near 277 nm.

The extreme proximity of the lowest $n\pi^*$ and $\pi\pi^*$-L_a state and the vicinity of the $\pi\pi^*$-L_b state have important implications for the excited state dynamics. For jet-cooled adenine, femtosecond pump–probe experiments produce a biexponential decay with $\tau_1 = 40$–100 fs and $\tau_2 = 0.75$–1.1 ps, depending on pump wavelength between 250 and 277 nm [35,56,124–127]. Canuel *et al*. observed $\tau_1 = 200$ fs upon substitution of the amino group H-atoms by methyl groups and interpreted this effect as deceleration of deactivation by a cutback of the vibronic coupling between $\pi\pi^*$ and $n\pi^*$ states due to the changes at the amino group and the pyrimidine ring out-of-plane vibrations [128]. Internal conversion then follows by $n\pi^*$-S_0 crossing at the conical intersection. With fs time-resolved photoelectron spectroscopy temporal evolution of the emitted electrons can be monitored and their kinetic energy measured simultaneously so that the motion of the wavepacket on the $n\pi^*$ and $\pi\pi^*$-surfaces can be followed separately. With this method, dynamics on the excited state surface can be analysed even at 250 nm pump wavelength at the maximum of adenine absorption where no discernible vibronic structure is observed. Stolow *et al*. found ultrafast L_a-$n\pi^*$ relaxation with $\tau_{La}<50$ fs and identified $n\pi^*$-ground state conversion with $\tau_{n\pi^*} = 750$ fs as the main de-excitation path at 250 nm excitation [129]. UV Resonance Raman spectroscopy provides complementary information to time-resolved techniques with data for the first 50 fs of excited state structural dynamics, as obtained from the resonance enhanced vibrations [130]. Oladepo and Loppnow reported lengthening of the ring double bonds towards single bonds is in 9-methyladenine and connected this to the formation of adenine photodimers [130].

When interpreting the fs broadband excitation results, one has to keep in mind the spectroscopic findings which show that adenine's lowest $n\pi^*$-state is optically active and can therefore also be populated at excitation wavelengths below 277 nm similar to the bright L_b state for which excitation below 275 nm cannot be neglected. Furthermore, the contribution of

the $\pi\sigma^*$ state at short excitation wavelengths is not completely clear yet [121,123]. Interpretation of fs results may thus be more complicated than hitherto assumed and requires further efforts.

What do dynamics calculations tell us about the nature of the CI in the adenine monomer? Most CI are characterised by a ring puckering of the pyrimidine ring, see Figure 3. The energetically lowest conical intersection was found on the crossing seam intersecting $\pi\pi^*$ and closed shell surfaces and it is, according to the Boeyens classification scheme [131], labelled as ^{2}E, characterised by a ring puckering of the pyrimidine ring at C2, followed by $^1S_6$ which corresponds to the minimum on the crossing seam of the $n\pi^*$ state and the ground state [4,47,132–135]. The CI is characterised by a strong out-of-plane displacement of the amino group. Additionally, Barbatti and Lischka found other structures, in particular, $^4S_3$ and B_{36} both of $n\pi^*$ and closed shell characters [135]. The conical intersection connected with the deformation of the imidazol ring is characterised by puckering at the C8 atom and it is located on the crossing seam of $\pi\pi^*$ and closed shell surfaces. Based on the relative energies, all but $^4S_3$ are accessible from the vertical FC region. Sobolewski *et al*. and Perun *et al*. reported a conical intersection associated with breaking of the CN and NH bonds [134,136,137].

Reaction paths calculated by Barbatti and Lischka suggest that the two lowest CI are the most effective since they are accessible from the vertical FC region by a barrierless descending path [135]. Based on the character of the PES, the authors propose a two-step process in the relaxation of adenine: an ultrafast step of 100 fs and an additional longer step of about 1 ps [47,115,134,138–141]. The fast process involves relaxation from the vertical FC region to the S_1 minimum, while the slower process corresponds to relaxation from the S_1 minimum to the ground state [115,134,138,139] via ^{2}E and $^1S_6$ CI at lower and higher excitations, respectively [138,139]. The relaxation taking place at higher excitation energies also proceeds via CI, characterised by bond breaking [137,142,143]. Serrano-Andres *et al*. [47] provided an alternative explanation of the relaxation mechanism according to which part of the population relaxes within 100 fs via a barrierless and a diabatic path at a ^{2}E conical intersection and the remaining population deactivates at longer time via a $^1S_6$ conical intersection.

Non-adiabatic dynamics simulations performed with the semi-empirical OM2 method suggest that the most important conical intersection is $^1S_6$ with the amino group strongly distorted from the plane [98]. Thiel *et al*. found that τ_{La} contains a minor contribution of direct L_a-gs de-excitation corresponding to the experimentally observed $\tau_{La}<50$ fs whereas most trajectories run through the L_a-$n\pi^*$ and $n\pi^*$-gs CIs corresponding to the observed $\tau_{n\pi^*}=750$ fs [98]. According to the interpretation reported by Barbatti and Lischka, the first step of adenine's dynamics corresponds to ultrafast relaxation from the S_3 to the S_1 state [98,144]. Within 60 fs, the vast majority of population is already in the S_1 state. Further relaxation from the S_1 state to the ground state takes about 1 ps. During the whole course of the dynamics, the authors did not observe any relaxation via the $^1S_6$ conical intersection. In fact, the trajectories utilise almost exclusively structures close to the ^{2}E conical intersection. Both CI should be accessible from the vertical FC region, as their energies are well below the excitation energy of the bright state and they are connected via reaction paths with no barrier. However, the more demanding geometrical rearrangements required to reach the $^1S_6$ potential are very likely the reason why this conical intersection was not observed. The fast step of the relaxation very likely proceeds via a three-state conical intersection as suggested by Matsika [145]. This suggestion is supported by the fact that in the vertical FC region the

energies of the S_1, S_2 and S_3 states are almost degenerate. The results of dynamics studies performed by Barbatti and Lischka [94] do not exclude the existence of a relaxation mechanism in which bond breaking takes place. This mechanism should be, however, efficient at higher initial energies only.

Monte Carlo/CASPT2 calculations point to CI connecting the $\pi\pi^*$ and $n\pi^*$ states of 9H-adenine to the ground state in aqueous solution as well, however due to the large destabilisation of the $n\pi^*$ state in water, deactivation occurs mainly via the $\pi\pi^*$ state leading to monoexponential decay [45,146–148].

4.3. *Thymine*

Absorption of UV radiation by DNA can generate mutations which mainly occur at bipyrimidine sites. Stacked thymine (T) sites react to form cyclobutane pyrimidine dimers in less than 1 ps [67,149] whereas a minor pyrimidine-(6–4)-pyrimidone adduct is formed within 4 ms probably via intermediate oxetane [150]. The ultrafast dimerisation occurs directly in the photoexcited $^1\pi\pi^*$ state [67,151] but there are contributions to dimer formation by a long-living $^1n\pi^*$ or triplet state [149,152,153] populated by internal conversion (IC). Intersystem crossing (ISC) from the $^1\pi\pi^*$ state seems to occur also [154–156], at least in a solution of nucleobases where monomer diffusion limits reaction time and requires long-living excited states. Triplet formation has a low quantum yield of <0.02 in aqueous solution [157–160] but is still interesting as possible precursor for dimer formation because T has the lowest triplet energy of all nucleobases [161] hence interbase triplet energy transfer would accumulate ^{3}T. Even non-concerted product formation via reaction of hot S_0 ground state nucleobases may contribute to dimer formation. The dominant T decay (~90%) is indeed sub-picosecond $^1\pi\pi^*$–S_0 conversion leading to hot T which cools within a few ps in water [46]. Vibrational relaxation, however, may be too fast and the reaction barrier in the ground state too high to allow a significant contribution of hot ground state reaction.

Spectroscopy of isolated T in the gas phase can help to solve the puzzle of thymine's excited states. IR and microwave experiments point to the diketo tautomer of uracile (U) and T as dominating species in the gas phase [162–164]. The electronic spectra of isolated U and T are broad and diffuse [162] consistent with the observed ultrafast decay times [46,165]. Nanosecond delayed ionisation experiments with 1-methylthymine (1MT) and 1-methyluracil (1MU) demonstrate the existence of a long-lived 'dark' electronic state alongside with the short-lived bright $^1\pi\pi^*$–state. Kong *et al*. concluded from their experiments on 1MT-water clusters that hydration accelerates internal $^1\pi\pi^*$–S_0 conversion to a degree that the long-lived dark state is not populated anymore and stated that short excited state lifetime and photostability is not an intrinsic property of the pyrimidine bases but results from their hydration [166]. On the other hand, Busker *et al*. [167] observed an increase of the dark state lifetime of 1MT– and 1MU-water clusters in the gas phase under careful control of the applied water pressure in agreement with the observation of a long-lived dark state upon UV excitation of T and U nucleotides in aqueous solutions [46]. Several authors tentatively assigned the dark state to the $n\pi^*$-state both in the gas [166,167] and condensed phase [46] with a triplet state as alternative. These proposals were mainly based on the observation of sub-microsecond lifetimes of the dark state in the gas phase and sub-nanosecond lifetimes in water, whereas lifetimes of many microseconds are typical for triplet states. Kunitsky *et al*. were able to measure a vibrational spectrum of the dark state of isolated 1mT in the NH/OH

stretch region [165] and, based on comparison with the calculated $^1n\pi^*$- and $^3\pi\pi^*$-NH stretch frequencies [168], assigned the spectrum to the lowest triplet state of the keto tautomer. From the dependence of the dark state ionisation rate on the laser intensity, they ruled out the hot electronic ground state. Triplet formation from the singlet state can indeed occur very effectively via large spin–orbit coupling if the two states have different spatial symmetry [169,170]. Etinski *et al*. [168] calculated sub-nanosecond $^1n\pi^*$–$^3\pi\pi^*$ intersystem crossing times for 1MT and T and, therefore, also suggested that the dark state has triplet multiplicity. The lowest triplet state of thymine and thymidine was detected via the triplet carbonyl stretch bands at 1603 and $\sim$1700 cm^{-1} with fs and ns UV-infrared pump–probe spectroscopy in acetonitrile solution [171]. The triplet state is formed in less than 10 ps and a vibrationally relaxed $^1n\pi^*$-state as triplet precursor was ruled out because the $^1n\pi^*$-state has a lifetime of $\sim$3 ns in acetonitrile for the closely related cyclohexyluracil and between 10 and 100 ps for different pyrimidine bases in aqueous solution. Hot $^1n\pi^*$ molecules, however, are possible precursors of triplet T in solution [46]. In the gas phase, the lifetime of the dark state detected by R2PI is a key parameter to determine its multiplicity. The triplet lifetime of T in acetonitrile solution is 10 μs in the absence of self-quenching [159] and comparable lifetimes are expected in the gas phase. Lifetimes of 227 ± 30 ns for carefully dried 1MT at the 1MT mass and >1.5 μs for water clusters detected at the 1-MT(H_2O) mass were observed [167]. Hence, the dark state lifetime of the 1MT monomer detected by R2PI is not in agreement with the expected intrinsic lifetime of triplet thymine while in the water clusters a triplet contribution cannot be excluded. Kunitski *et al*. measured a lifetime of 340 ± 50 ns for 1MT, similar to 363 ± 30 ns at the 1MT mass in the presence of water [167], pointing to a contribution from fragmenting 1MT-water clusters to the delayed ionisation signal [165].

What do dynamics calculations tell us about the CI in excited thymine which give rise to its ultrafast internal conversion and broad electronic spectrum? Contrary to cytosine, the bright state of $\pi\pi^*$ character in the vertical FC region of thymine is the S_2 state. The S_1 and S_2 minima were found to be of $n\pi^*$ and $\pi\pi^*$ character, respectively. To explore the relaxation dynamics, Hudock *et al*. and Szymczak *et al*. [92,172] investigated minima on the crossing seams of S_2 with S_1 as well as S_1 with S_0 [8,103,172]. For the former, the lowest energy structure was found to have a boat conformation, labelled according to Boeyens classification as B_{36} [92,172]. For the later, the low-lying CI are reached by rotating along the C5–C6 bond with the largest puckering at the C5 atom and out-of-plane distortion of the methyl group and the C6 atoms (^6E and ^5E) [8,103]. Both pathways are characterised by the $\pi\pi^*$/closed-shell character of the wavefunction. These two structures are followed by a B_{41} conical intersection with out-of-plane distortion of the oxygen and $n\pi^*$/closed-shell character of the wavefunctions.

The longer lifetime of about 5 ps was interpreted with three different scenarios: (i) Perun *et al*. suggested that trapping in the minimum of the S_1 state of $n\pi^*$ character is the reason for a longer lifetime [173]. (ii) Dynamics simulations run with the multiple spawning method showed only a very small fraction of trajectories which would deactivate to the S_1 state within 500 fs [92]. Based on this finding, trapping in the S_2 state was invoked to explain the experimentally observed longer lifetime of thymine. However, this trapping in the S_2 state was not observed in the dynamics simulations performed at the semiempirical OM2 level [97]. (iii) The third scenario, suggested by Merchan *et al*. [10] for all pyrimidine-based molecules, predicts that after excitation to the S_2 state the molecules either follow a barrierless path toward the S_1/S_0 conical intersection or get trapped in the S_2 state. The former

mechanism was associated with the relaxation lifetime on the femtosecond timescale, while the later corresponds to the longer lifetime.

Dynamics simulations performed at the CASSCF level, run for a longer simulation time, showed that after excitation thymine quickly relaxes from the vertical FC region to the S_2 state of $\pi(O)\pi^*$ character where it remains for about 2.5 ps [172]. The crossing seam which intersects the S_2 and S_1 states at the CI is characterised as a B_{36} conformation. This interpretation is in agreement with the results suggested by Hudock *et al*. [92]. The simulation time used in this study does not encompass the additional relaxation process from the S_1 state to the ground state. Based on the results reported in reference [103], this step can also take a relatively long time. Either the ascending character of the pathways or the barrier along the reaction paths found in this study could be responsible for a smaller efficiency of these trajectories through the CI.

4.4. *Uracil*

The character of the spectrum in the vertical FC region and the minima on the S_1 and S_2 surfaces of uracil (U) are very similar to those of thymine. The characters of the energetically lowest S_2/S_1 CI are also very similar, with a boat conformation and the wavefunction characterised by mixing of $n\pi^*/\pi\pi^*$ electronic configurations [53,92,174]. The S_1/S_0 CI are also very similar to those found in thymine, although their minimisation led to slightly different Boeyens characterisations. In particular, these are ethylenic biradical structures with puckering at the C6 and/or C5 atoms, labelled as E_6 and $^6S_5$, and a boat conformation with out-of-plane distortion and $n\pi^*$/cs electronic structure [97,175]. In addition, an open-ring conical intersection was found at low energy. Although the static calculations show very similar character of the critical points of the PES, i.e. excited state minima and CI, including their relative energies, the experimentally observed lifetimes are significantly different. 'Static calculations' led to the same predictions of relaxation mechanisms as those suggested for thymine, i.e. (i) a direct path of $\pi\pi^*$ character to the ethylenic conical intersection [8,10,174], (ii) a relaxation path which includes trapping in the S_1 minimum of $n\pi^*$ character [174,176] and (iii) trapping in the S2 minimum [92]. Dynamics calculations based on the multiple spawning method predict trapping in the S_2 state to dominate the relaxation of uracil [92] while semi-empirical OM2 simulations predict an indirect decay mechanism which includes the *oop*-O conical intersection [97].

To explore the photodynamics of uracil and compare it to thymine, Nachtigallová *et al*. performed dynamics simulations with the same conditions as those used for thymine [175]. The following picture emerges: the main relaxation mechanism is characterised by trapping of the molecule in the S_2 minimum of $\pi(O)\pi^*$ character. This mechanism was observed for 55 and 77% of trajectories, run with the excitation energies at the maximum of the absorption peak and slightly below, respectively. For this relaxation mechanism, time constants of 1.5 and 1.8 ps (depending on the pump energy) were determined which could explain the longer decay constant observed experimentally. The remaining trajectories do not get trapped in the S_2 state. In fact, they quickly reach the S_1 state from which they relax to the ground state either via a direct $\pi\pi^*$ relaxation path, preferentially via an ethylenic CI puckered at the C6 atom, or via a ring-opening CI. In the latter case, a $n\pi^*$ electronic configuration mixes into the final wavefunction in the relaxation process. Existence of this direct mechanism, not observed for thymine, is very likely the reason for the shorter lifetime of uracil compared to

thymine. The estimated decay constant for this mechanism is about 0.7 ps, explaining the shorter decay constant.

Barbatti *et al*. employed dynamics studies of the excited state behaviour of all five nucleobases, described at comparable level of theory and under conditions relevant to experiments, to systematically compare purine- and pyrimidine-based nucleobases [95]. This comparison shows that the relaxation mechanism of the purine-based nucleobases adenine and guanine is based on a diabatic $\pi\pi^*$ reaction path. The relaxation proceeds directly from the vertical FC region without trapping in any excited state minima. Contrary to this, pyrimidine-based nucleobases – cytosine, uracil and thymine, show more complex relaxation mechanisms which include both $n\pi^*$ and $\pi\pi^*$ relaxation pathways as well as trapping in either the S_1 or the S_2 minimum.

Nachtigallová *et al*. have measured lifetimes in the nanosecond regime for individual tautomers of five-substituted uracils, U, which provide an interesting case for investigating the role of the solvent, see Figure 4 and discussion above [5]. Interestingly, 5-aminouracil (5AU) has been reported to act as an antitumor, antibacterial and antiviral drug [177–179]. According to their quantum computational modelling, the big difference in excited state lifetimes indicated in Figure 4 can be explained by the relevant $\pi\pi^*$ and $n\pi^*$ states switching in energy in the FC region. The behaviour in bulk water is rather different. In bulk water, 5AU (200 fs) lives just twice as long as U (100 fs) but dimethylaminouracil, DM5AU, has a long-lived component ($\sim$100 ps) [180]. A possible explanation is that the effect of the water is largest through hydrogen bonding to the amino group, which is blocked in DM5AU. This would explain why the behaviour of DM5AU in solution resembles that of 5AU in the gas phase.

4.5. Cytosine

The amino-keto tautomer of cytosine shows ultrafast excited state decay time constants of <50 fs, 820 fs and 3.2 ps upon excitation at 250 nm, see Figure 4 and reference [56]. The R2PI spectrum consists of just a few lines around 313 nm indicating a longer lifetime in this spectral region [58]. Again decay times from dynamics calculations can be correlated to the measured lifetimes and shine light on the CIs responsible for the ultrafast deactivation.

The vertical excitation energy of the first bright excited state is of $\pi\pi^*$ character and the S_1 minimum of $n\pi^*$ character. Barbatti *et al*. [181] found three CI on the crossing seams with the ground state, labelled as (i) *semi-planar*, characterised by a wavefunction with mixed $n\pi^*$, $\pi\pi^*$ and ground stated electronic configurations; (ii) *oop*-NH_2 with out-of-plane displacement of the amino group and an $n\pi^*$ electronic configuration in the wavefunction and (iii) a C6-*puckered* conical intersection with twisting of the C5–C6 bond, puckering of the C6 atom and a wavefunction with a $\pi\pi^*$ electronic configuration. The *semi-planar* and *oop*-NH_2 intersections were first reported by Ismail *et al*., the C6-*puckered* was reported by Sobolewski and Domcke and Zgierski *et al*. [182–185]. All these CI are accessible from the vertical FC region.

Based on energetic considerations, in particular the barrierless connection of the vertical FC region and the C6-*puckered* conical intersection, a direct relaxation via this conical intersection was predicted by Merchan and Serrano-Andress [10,11]. This prediction was supported by surface hopping dynamics simulations performed at the semi-empirical OM2 level. Contrary to this model, the results of dynamics simulations performed with multiple spawning at the CASSCF(2,2) level [93] and surface hopping [100] at the AM1/CI level predict that only a small fraction of trajectories follows this reaction channel, while the

oop-NH2 conical intersection dominates the relaxation. Additionally, results obtained with multi-reference CASSCF wavefunctions with larger active space show that the *semi-planar* crossing seam should be the most important [186].

Dynamics simulation studies performed by Barbatti *et al*. at the CASSCF level show that the relaxation mechanism is more complicated [181]. The dynamics was run for 1.2 ps. The suggested mechanism is as follows: from the vertical FC region, the system follows the $\pi\pi^*$ state and almost instantly reaches the region of strong mixing of $\pi\pi^*$, $n\pi^*$ and closed shell electronic configurations. A small part of the population (about 16%) relaxes directly from this region to the ground state within 13 fs. The majority of trajectories (84%) first relax to the S_1 minimum with $n\pi^*$ character, from where they can convert to the ground state via three different pathways. About 62% of the population relaxes from this minimum following a path of $n\pi^*$ character and relaxing via a *semi-planar* conical intersection of the same electronic character. The remaining 18% follows the $\pi\pi^*$ state either via C6-*puckered* or *oop*-NH_2 CI. These mechanisms are responsible for the relaxation decay with the intermediate decay constant. Besides, 20% of trajectories which do not relax within the simulation time can contribute to the longer time constant of 3 ps observed in the experiment. This interpretation agrees with the three different experimentally observed relaxation time scales.

5. Interactions between bases

5.1. *Base pairing*

5.1.1. *Stacking vs. hydrogen bond base pairing*

Two types of non-covalent interactions are prevalent in DNA: hydrogen bonding and base stacking. Both interactions are important with hydrogen bonding providing the recognition mechanism and base stacking providing most of the structural stabilisation. A possible different response to UV excitation in these two structural motifs is intriguing for modelling prebiotic chemistry: what came first, recognition or formation of a macromolecule?

In solution phase experiments, Crespo-Hernández, Kohler, and co-workers have shown that base stacking in single- and double-stranded DNA favours non-radiative decay via the formation of CT or exciplex states [187–189]. Such states decay much more slowly than the $\pi\pi^*$ states in single bases. The authors studied single homopolymeric strands in solution, which exhibit partly stacked structures. In transient absorption, they observed both ultrafast ($\tau \approx 1$ ps) decay – ascribed to unstacked parts of the structure – and decay at a two orders of magnitude slower scale – attributed to stacked regions in the structure [190]. Double-stranded helices, containing both the stacking and the base pairing motifs, show the same slower decay as the single strands, suggesting that the dynamics in this case is dominated by *intra*strand rather than by *inter*strand interactions [187]. Work by Takaya *et al*. suggests that regardless of sequence length, initial excitons trap to a common state that is localised on just two bases [188]. In their model, rapid decay then takes place to exciplexes, followed by charge recombination on a picosecond timescale.

For single bases in the gas phase, hydrogen bonding generally dominates while stacking is prevalent only in solution; see the stacked 9MA-A clusters discussed below and Kim *et al*. [191] as an exception. According to Hobza and Sponer, it requires on the order of three to six water molecules, depending on the specific base pair, to stabilise stacking between two isolated bases [192]. Saigusa and co-workers have recently shown that GG dimers and

methyl-substituted GC clusters with one water molecule form the same hydrogen-bonded structures as without the water molecule and they saw no evidence of stacking similar to earlier findings by Mons *et al*. and Abo-Riziq *et al*. and Oiuzzi *et al*. [193–195].

In xanthine model systems in the gas phase, Callahan *et al*. show the stacking to be competitive with hydrogen bonding upon a single methylation and to be dominant upon two methylations [196]. For 3,7-dimethylxanthine dimers stacking is observed exclusively, although the first hydrogen-bonded structure is calculated to be only 2.6 kcal/mol higher in energy while 1,7-dimethylxanthine dimers are not observed at all. Figure 8 shows the stacked structure of trimethylxanthine dimers.

5.2. *Guanine–cytosine*

The subtle role of interbase hydrogen bonding in excited state dynamics is demonstrated in the example of isolated GC base pairing [197]. Of the about 50 possible ways to form GC base pairs by hydrogen bonding, the one structure that is prevalent in DNA (the Watson–Crick (WC) structure) has a sub-picosecond excited state lifetime, evidenced by a broad UV spectrum, while other structural arrangements of the same base pair have sharp spectra, consistent with much longer excited state lifetimes [197]. Sobolewski and Domcke have proposed that relaxation occurs by ultrafast transfer of a shared proton within the base pair [198,199]. Light-induced proton transfer is a common mechanism exploited in UV stabilisers [200]. Similar effects appear in other base pair combinations like isolated GG and CC where the lowest energy structures could not be detected by R2PI [57,201,202].

Figure 9 shows the proposed reaction path for ultrafast internal conversion of guanine–cytosine base pairs in the gas phase, involving excited state proton transfer (ESPT). A barrierless conical intersection (CI) connects the bright $^1\pi\pi^*$ states, mainly delocalised on G and C, with an excited state with $G \rightarrow C$ CT character. The CT state is massively stabilised by a $G^+ \rightarrow C^-$ ESPT reaction leading to a diradical (GC_{dir}) state (G–H) (C+H) with an easily accessible CI to the electronic ground state of GC [183,198]. In the gas phase, ultrafast ESPT is the main path for internal conversion to the S_0 state in the GC WC pair [183,197,198,204–206] and has been proposed to be dominating in $CHCl_3$ solution too [207,208] based on fs fluorescence up-conversion experiments. In a recent paper, Improta *et al*. demonstrated by broad-band transient absorption spectroscopy and TD-DFT/CAM-B3LYP calculations in solution that GC ESPT is not effective in $CHCl_3$ [203]. The kinetics of the combined monomer (G + C) and dimer (GC) broadband transient spectra is extremely similar at <2 ps and shows only slight differences from 2 to 100 ps. Thus relaxation in the monomer moieties dominates internal conversion of GC in solution. Calculations show that even a weakly polar solvent like $CHCl_3$ lowers the energy of the GC_{CT} state significantly

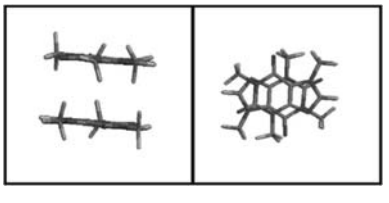

Figure 8. Stacked structure of trimethylxanthine dimer based on a molecular dynamics simulation.

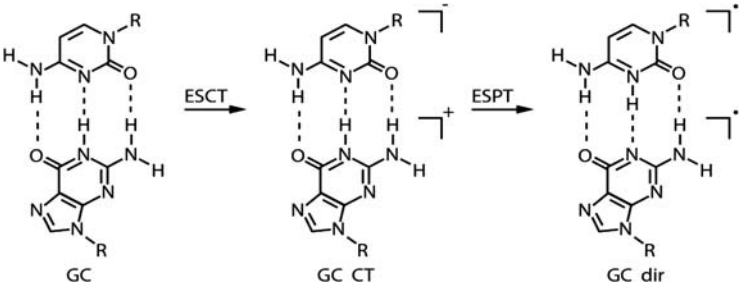

Figure 9. The isolated GC WC dimer easily converts from the optically excited $^1\pi\pi^*$ state to the dark G → C CT state and transfers a proton to obtain a diradical species GC–dir with an energy very close to a CI with S_0. In solution, this path is closed and ESPT is not involved in the ultrafast deactivation of GC to the electronic ground state. Figure is adapted from Reference [203].

(∼0.8 eV) below the $G\pi\pi^*$ state so that $GC\pi\pi^* \rightarrow GC_{CT}$ is rendered ineffective. Furthermore in $CHCl_3$, a pronounced energy barrier of ∼0.3 eV separates GC_{CT} and GC_{dir}. The gap between the GC_{dir} minimum and S_0 is more than 1 eV along the whole NH···N reaction path. Proton transfer implies the quenching of the strong dipole moment of the CT state and this process is therefore not favoured even in a moderately polar surrounding.

GC polynucleotides also do not decay to the ground state faster than their monomer components [209,210]. Instead in GC rich polynucleotides, the excited state decay is probably controlled by the formation of intrastrand exciplexes. GC and GG stacking in the DNA helix may lead to CT, ESPT and finally internal conversion to the ground state. The characteristic UV spectrum of the (G–H) radical [211] was indeed observed [212] in large GG aggregates in hexane where hydrogen-bonded G ribbons are formed [212,213]. GC aggregates in hexane did not show formation of the (G–H) radical.

5.3. *Adenine–thymine*

The IR–UV spectrum of the AT base pair in the gas phase was assigned to cluster structures with HNH···O=C/N···HN hydrogen bonds [214]. The observed experimental spectrum does not agree with the vibrational spectrum of the WC AT structure. Ab initio calculations indeed show that the WC isomer is not the most stable AT arrangement [214]. Obviously the DNA backbone enforces the AT WC arrangement. Other more stable configurations are possibly blocked by the sugar substitution or other steric or electronic reasons. Solvent effects on electron driven proton transfer in AT WC pairs are discussed by Dargiewiscz *et al*. [215].

Adenine is known to form long-lived exciplex states via π-stacking which decisively determine its excited state dynamics in DNA [188]. High-resolution spectroscopy in the gas phase allows very detailed studies of the excited states of A–A aggregates. Indeed, in the case of 9-methyladenine(9MA)-adenine(A), a stacked structure was observed with an IR–UV spectrum pointing to one free NH_2 and N9H group and one only weakly interacting NH_2 group [216]. Interestingly extensive H-transfer was observed in the stacked excited A–A dimer probably via $N9H(A) \rightarrow NH_2(9MA)$. The electronic spectrum could only be observed at the 9MA+H mass and not at the parent mass. The 9MA-A is the only nucleobase cluster to date for which a stacked structure has been observed in the gas phase.

5.4. *Alternate base pairs*

Numerous studies have proposed possible alternate base pair combinations that could suggest credible alternatives to the canonical base pairing scheme in terms of stability and recognition [217]. Benner and co-workers, for example, have proposed an 'alternate genetic lexicon' formed by merely exchanging the hydrogen donor and acceptor groups in the base pair structures [218]. If the canonical bases were present in a primordial soup, it is reasonable to assume that all other derivatives and analogues were present as well [219]. As an example of an alternate base pair, geometrically equivalent to guanine-cytosine, Gengeliczki *et al*. have obtained the structure of clusters of 2,4-diaminopyrimidine with 3,7-dimethylxanthine in the gas phase [220]. They reported the four lowest energy structures, which include the WC base pairing motif. This WC structure has not been observed by nanosecond R2PI in the gas phase for the canonical DNA base pairs. This finding raises the intriguing question whether such alternate base pairs may have longer excited state lifetimes and thus be less robust under UV irradiation. If indeed that is the case, it would be consistent with a chemical selection of the molecular building blocks of life on an early earth.

5.5. *Other interactions*

5.5.1. *Base–amino acid interaction*

The details of the interactions between proteins and DNA and the resulting recognition mechanisms are not understood in detail at the molecular level. The non-covalent forces that appear to govern such interactions are weak, and yet binding to certain sequences can be very specific. In fact, binding to specific sites can sometimes be orders of magnitude stronger than binding to random sites. Crews *et al*. studied guanine aspartic acid clusters as a very simple model system and identified structures and binding motifs [221].

5.5.2. *Base stacking, exciplex formation and photochemistry*

Contrary to single nucleobases and their mononucleotides which generally have excited $\pi\pi^*$ states with lifetimes of less than 1 ps and some, often minor, branching to longer lived $^1n\pi^*$ and triplet states, dinucleotides and polybase strands have lifetimes of 10–100 ps [188] and longer [222,223]. The yield of these long-lifetime species is 20–30% and thus similar to the fraction of stacked bases determined by NMR and CD measurements [149,188]. Obviously electronic coupling between adjacent bases drastically slows the excited state relaxation. The lifetime of the long-lived states increases with increasing energy of the base$^+$–base$^-$ CT state in accord with the well known slowing down of charge recombination with energy of the radical-ion exciplex. Hence, the following picture emerges. Initially, Frenkel excitons delocalised over several bases give rise to the strong UV absorption of DNA strands [224]. These initial bright states trap to long-lived states localised on pairs of stacked bases, see Figure 10. In a geometrically suitable arrangement electron transfer can take place with high efficiency and exciplex states ($B_1^+B_2^-$ in Figure 10) are formed which relax via charge recombination on the 10–100 ps time scale to B_1B_2 [188].

Femtosecond UV–IR pump–probe experiments show that cyclobutan dimer (CPD) formation in single-stranded all-thymine oligonucleotides takes only ~1 ps and therefore crucially depends on the proper π stacking orientation at the instant of excitation [67,225–228]. This

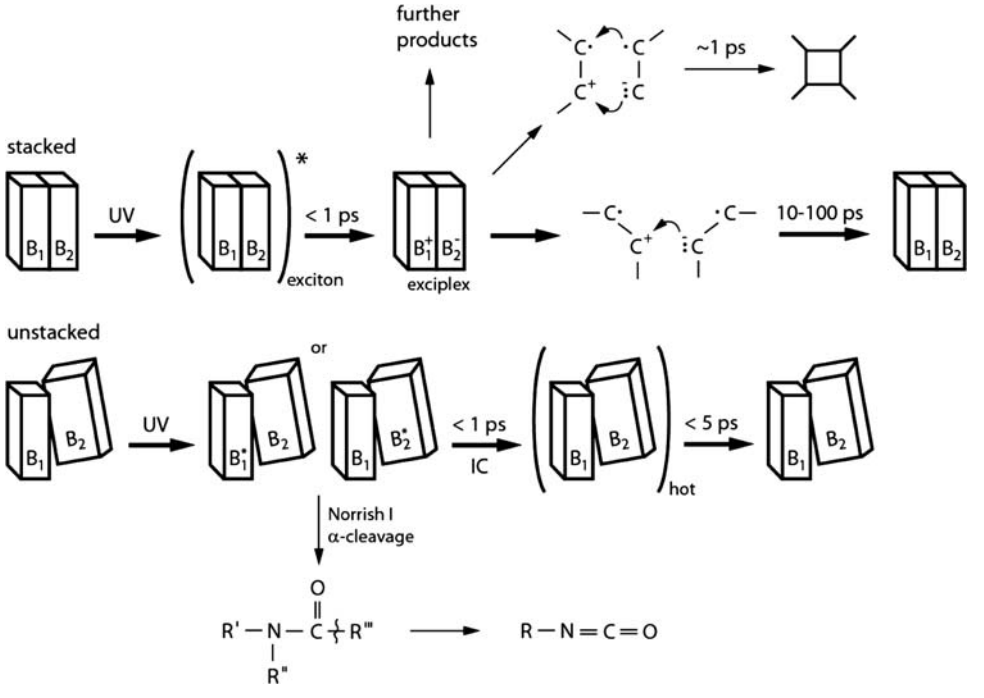

Figure 10. Exciplex formation in stacked bases B in DNA strands. Appropriate π stacking orientation at the instant of excitation leads to cyclobutane formation while other orientations merely lead to relaxation via charge recombination. Norrish type I α-cleavage can occur in DNA strands as well as in mononucleotides containing nucleobases with carbonyl groups. Part of the figure is adapted from reference [188].

exact geometry however is a rare event explaining the low quantum yield of CPD formation in thymine strands and thymine containing DNA. Similar to TT stacks, packed AT in UV-C-irradiated double-stranded DNA reacts to cyclobutane adducts which fragment to different products [149,229]. The explanation of the mechanism of cycobutane formation based on the multi-configurational CASSCF/CASPT2 description was provided for two adjacent cytosines [230] and thymines [231].

While adduct formation can only take place in stacked bases, Norrish type I α-cleavage can occur in mononucleosides as well. UV-induced ring opening was observed by Lapinski *et al*. in 1-methyl-2(1H)-pyrimidone as well as in 1-methylcytosine and tentatively assigned by IR matrix isolation spectroscopy via detection of the characteristic intense –N=C=O (isocyanate) stretch vibration at 2263 and 2261 cm^{-1} [232]. The 266 nm irradiation of dry films of dG_{10}, dC_{10} and dT_{10} strands and G, C and T derivatives also leads to ring opening and isocyanate formation [233]. Light of a broad-band UV lamp with sun intensity also introduces this reaction for instance in dT_{10} films and in G derivatives in hexane. Norrish cleavage in dG_{10}–dC_{10} double strands is less efficient [233]. It is tempting to connect the observed Norrish type I α-cleavage to the weakening of the conjugated double bond system in the pyrimidine ring both in the lowest $\pi\pi^*$- and $n\pi^*$ state leading to ring distortions. UV-induced

amino-oxo to imino hydrogen transfer was observed in matrix-isolated 1-methylcytosine and in G and C containing oligonucleotides [233,234].

The detailed computational understanding of the nature of electronically excited nucleic acid bases interacting via stacking and the effect of base sequence and nucleic acid conformation is still a considerable challenge due to its complexity [13,48,187,230,231,235–245]. In principle, these interactions can result in the population of locally excited states, delocalised exciton states, energy transfer and excimer formation.

Calculations have been performed to compute the electronic coupling in terms of both contributing mechanisms, i.e. short-range interactions due to the orbital overlap and the Coulombic interactions, operating over larger through space distances [239,246–251].

Various models and computational methods have been used to explore the character of delocalisation of the excited states among several nucleobases [239,246,252–256] focusing mainly on CT character during the formation of delocalised excitons and excimers and effects of structure fluctuations within the DNA molecule.

Nachtigallová *et al*. performed nonadiabatic dynamic simulations of the model system of 4-aminopyrimidine to explore effects of steric constraints on photodynamic behaviour of adenine [257]. They showed that these constraints do not significantly affect the relaxation mechanism. In addition, the intrastrand hydrogen bonds formed during the 4-aminopyrimidine photodynamics make the relaxation mechanism faster. The same effects were found also for the photodynamic behaviour of 4-aminopyrimidine embedded within double-stranded DNA [258]. Based on the calculations on $(dA)_{10}.(dT)_{10}$ oligonucleotide, Conti *et al*. [259] suggested that the formation of minimal energy complexes between two nucleobases is the source of a steric hindrance of out-of-plane motion of relaxing nucleobase, increasing its excited state lifetime.

Nonadiabatic dynamics simulations on adenine in a DNA environment were performed by Thiel and co-workers [260,261]. Using the model of $(dA)_{10}$ and $(dA)_{10}.(dT)_{10}$ oligomers, simulation times for relaxation to the ground state of several picoseconds were observed, which is about an order of magnitude longer than those found for isolated adenine. While two major channels decay via $^{6}S_1$ and ^{2}E CI in the case of the single stranded $(dA)_{10}$ oligomer, the former is completely blocked by hydrogen bonding between thymine and adenine in the $(dA)_{10}.(dT)_{10}$ oligomers.

Computational studies on $(9\text{-methyl-adenine})_2$ $(1\text{-methyl-thymine})_2$ stacked tetramer were performed with the TD-DFT method in aqueous solution. These calculations suggest that originally delocalised excitation is quickly localised on a single monomer giving rise to monomer like behaviour characterised by ultrafast relaxation [252]. The slower decay channels are devoted to the formation of excimers between two stacked adenines which according to Santoro *et al*. are of CT character. Neutral excimers are assumed to be formed in single strand DNA structures [262,263]. In strongly distorted geometries of single-strand DNA, the stability of neutral excimers is predicted to be comparable with the stability of CT excimers.

The formation of adenine aggregates formed in single-stranded adenine was confirmed also in studies by Hu *et al*. [264] using the TD-DFT method. In agreement with the work of Improta, they observed formation of states delocalised over several bases [265].

6. Summary and outlook

The picture that emerges is that the excited state dynamics of purines and pyrimidines depends critically both on intramolecular and intermolecular structure. The shape of the excited state potential determines the outcome following excitation. Ultrafast internal conversion involves trajectories on the potential surfaces via CI and the potential energy landscape varies in subtle ways between tautomers and derivatives. Non-covalent interactions with other molecules further complicate the situation, providing additional pathways for deactivation, such as proton transfer and exciton formation. The isolated molecules have been studied in great detail in the gas phase, including tautomer selective spectroscopy. This approach provides the best comparison with the highest level of theory, thus providing tests of algorithms, functionals and force fields. Gas phase studies also provide insights in very fundamental properties, but at the same time such results are incomplete because they omit the role of the environment. The latter is mostly studied in solution with femtosecond techniques. Experimentally a bridge between those two domains is formed by cluster studies. By combining insights gained in these different approaches an increasingly detailed understanding of DNA base excited state dynamics is being formed.

This field has benefited from simultaneous advances in experimental and computational techniques. In both areas, molecules of increasing size can be studied with increasing precision. One such new development is the ability to study ions in cold traps, providing dramatically improved spectroscopic resolution for larger compounds [66,266]. Additional progress may still be expected with further developments in all areas, which will hopefully lead to a completion of the reductionist journey from the properties of individual nucleobases to those of the macromolecule in its biological environment. This exploration is promising to lead to a comprehensive picture of DNA excited state dynamics and its implications for photochemical reactivity and stability.

Acknowledgements

The research at IOCB was part of the project RVO: 61388963. DN acknowledges the support from the Grant Agency of the Czech Republic (P208/12/1318). This material is based upon work supported by the National Science Foundation under CHE-0911564 and by NASA under NNX12AG77G. KK acknowledges the support from the Deutsche Forschungsgemeinschaft (SFB 663 and Kl 531-29)

References

[1] S. Matsika, Chem. Phys. **349**(1–3), 356 (2008).
[2] K. A. Kistler and S. Matsika, J. Phys. Chem. A **111**(14), 2650 (2007).
[3] C. M. Marian, J. Phys. Chem. A **111**(8), 1545 (2007).
[4] C. M. Marian, J. Chem. Phys. **122**(10), 10 (2005).
[5] D. Nachtigallová, H. Lischka, J. J. Szymczak, M. Barbatti, P. Hobza, Z. Gengeliczki, G. Pino, M. P. Callahan, and M. S. de Vries, PCCP **12**(19), 4924 (2010).
[6] M. S. de Vries, A. M. Rijs, B. O. Crews, J. S. Hannam, D. A. Leigh, M. Fanti, F. Zerbetto, and W. J. Buma, Angew. Chem. Int. Ed. **47**(17), 3174 (2008).
[7] R. Nandagopal, N. Sinaii, N. A. Avila, R. C. Van, W. Chen, G. P. Finkielstain, S. P. Mehta, N. B. McDonnell, and D. P. Merke, Eur. J. Endocrinol. **164**, 977 (2011).
[8] M. Z. Zgierski, S. Patchkovskii, T. Fujiwara, and E. C. Lim, J. Phys. Chem. A **109**(42), 9384 (2005).

[9] L. Serrano-Andrés, M. Merchan, and A. C. Borin, J. Am. Chem. Soc. **130**(8), 2473 (2008).
[10] M. Merchan, R. Gonzalez-Luque, T. Climent, L. Serrano-Andres, E. Rodriuguez, M. Reguero, and D. Pelaez, J. Phys. Chem. B **110**(51), 26471 (2006).
[11] M. Merchan and L. Serrano-Andres, J. Am. Chem. Soc. **125**(27), 8108 (2003).
[12] C. T. Middleton, K. de La Harpe, C. Su, Y. K. Law, C. E. Crespo-Hernandez, and B. Kohler, Annu. Rev. Phys. Chem. **60**, 217 (2009).
[13] C. E. Crespo-Hernandez, B. Cohen, P. M. Hare, and B. Kohler, Chem. Rev. **104**(4), 1977 (2004).
[14] M. S. de Vries and P. Hobza, Annu. Rev. Phys. Chem. **58**, 585 (2007).
[15] J. -E. A. Otterstedt, J. of Chem. Phy. **58**, 5716 (1973).
[16] M. Segado, M. A. Carvajal, I. Gomez, and M. Reguero, Theor. Chem. Acc. **128**(4–6), 713 (2011).
[17] S. Tommasi, M. F. Denissenko, and G. P. Pfeifer, Cancer Res. **57**(21), 4727 (1997).
[18] R. J. Malone, A. M. Miller, and B. Kohler, Photochem. Photobiol. **77**(2), 158 (2003).
[19] A. Broo, J. Phys. Chem. A **102**, 526 (1998).
[20] J. Andreasson, A. Holmen, and B. Albinsson, J. Phys. Chem. B **103**, 9782–9 (1999).
[21] N. J. Kim, G. Jeong, Y. S. Kim, J. Sung, S. K. Kim, and Y. D. Park, J. Chem. Phys. **113**(22), 10051 (2000).
[22] S. K. Mishra, M. K. Shukla, and P. C. Mishra, Spectrochimica Acta, Part A (Molecular and Biomolecular Spectroscopy) **56A**, 1355 (2000).
[23] D. C. Lührs, J. Viallon, and I. Fischer, Phys. Chem. Chem. Phys. **3**(10), 1827 (2001).
[24] H. Kang, B. Jung, and S. K. Kim, J. Chem. Phys. **118**(15), 6717 (2003).
[25] A. L. Sobolewski and W. Domcke, Eur. Phys. J. D **20**, 369 (2002).
[26] C. Plützer and K. Kleinermanns, PCCP **4**(20), 4877 (2002).
[27] C. Plützer, E. Nir, M. S. de Vries, and K. Kleinermanns, PCCP **3**(24), 5466 (2001).
[28] M. Barbatti and H. Lischka, J. Phys. Chem. A **111**(15), 2852 (2007).
[29] I. Hünig, C. Plützer, K. A. Seefeld, D. Löwenich, M. Nispel, and K. Kleinermanns, Chem. Phys. Chem. **5**(9), 1427 (2004).
[30] M. Zierhut, W. Roth, and I. Fischer, PCCP **6**(22), 5178 (2004).
[31] G. Zechmann and M. Barbatti, Int. J. Quantum Chem. **108**(7), 1266–76 (2008).
[32] Z. Gengeliczki, M. P. Callahan, N. Svadlenak, C. I. Pongor, B. Sztaray, L. Meerts, D. Nachtigallová, P. Hobza, M. Barbatti, H. Lischka, and M. S. de Vries, PCCP **12**(20), 5375 (2010).
[33] M. Kabelac, C. Plützer, K. Kleinermanns, and P. Hobza, PCCP **6**(10), 2781 (2004).
[34] D. Shemesh, A. L. Sobolewski, and W. Domcke, PCCP **12**(19), 4899 (2010).
[35] C. Canuel, M. Mons, F. Piuzzi, B. Tardivel, I. Dimicoli, and M. Elhanine, J. Chem. Phys. **122**(7), 074316 (2005).
[36] Y. Lee, M. Schmitt, K. Kleinermanns, and B. Kim, J. Phys. Chem. A **110**(42), 11819 (2006).
[37] E. Quinones and R. Arce, J. Am. Chem. Soc. **111**(21), 8218 (1989).
[38] R. W. Wilson and P. R. Callis, Photochem. Photobiol. **31**, 323–7 (1980).
[39] T. Gustavsson, A. Banyasz, E. Lazzarotto, D. Markovitsi, G. Scalmani, M. J. Frisch, V. Barone, and R. Improta, J. Am. Chem. Soc. **128**(2), 607–19 (2006).
[40] T. Gustavsson, N. Sarkar, E. Lazzarotto, D. Markovitsi, and R. Improta, Chem. Phys. Lett. **429**(4–6), 551 (2006).
[41] K. Seefeld, R. Brause, T. Häber, and K. Kleinermanns, J. Phys. Chem. A **111**(28), 6217 (2007).
[42] D. Nachtigallová, P. Hobza, and V. Spirko, J. Phys. Chem. A **112**(9), 1854 (2008).
[43] M. Mons, F. Piuzzi, I. Dimicoli, L. Gorb, and J. Leszczynski, J. Phys. Chem. A **110**(38), 10921 (2006).
[44] J. Cerny, V. Spirko, M. Mons, P. Hobza, and D. Nachtigallová, PCCP **8**(26), 3059 (2006).
[45] T. Pancur, N. K. Schwalb, F. Renth, and F. Temps, Chem. Phys. **313**(1–3), 199 (2005).

[46] P. M. Hare, C. E. Crespo-Hernandez, and B. Kohler, Proc. Nat. Acad. Sci. U.S.A. **104**(2), 435 (2007).
[47] L. Serrano-Andres, M. Merchan, and A. C. Borin, Proc. Nat. Acad. Sci. U.S.A. **103**(23), 8691 (2006).
[48] J. J. Serrano-Perez, I. Gonzalez-Ramirez, P. B. Coto, M. Merchan, and L. Serrano-Andres, J. Phys. Chem. B **112**(45), 14096 (2008).
[49] L. Serrano-Andres and M. Merchan, J Photoch Photobio C **10**(1), 21 (2009).
[50] K. A. Kistler and U. J. Matsika, J. Chem. Phys. **128**(21) (2008).
[51] K. A. Kistler and S. Matsika, J. Phys. Chem. A **111**(35), 8708–16 (2007).
[52] S. Yarasi, P. Brost, and G. R. Loppnow, J. Phys. Chem. A **111**(24), 5130 (2007).
[53] E. Epifanovsky, K. Kowalski, P. D. Fan, M. Valiev, S. Matsika, and A. I. Krylov, J. Phys. Chem. A **112**(40), 9983 (2008).
[54] S. Matsika and K. A. Kistler, J. Phys. Chem. A **111**(14), 2650 (2007).
[55] D. Markovitsi, T. Gustavsson, and I. Vaya, J. Phys. Chem. Lett. **1**(22), 3271 (2010).
[56] S. Ullrich, T. Schultz, M. Z. Zgierski, and A. Stolow, PCCP **6**(10), 2796 (2004).
[57] E. Nir, I. Hünig, K. Kleinermanns, and M. S. de Vries, PCCP **5**(21), 4780 (2003).
[58] E. Nir, M. Muller, L. I. Grace, and M. S. de Vries, Chem. Phys. Lett. **355**(1–2), 59 (2002).
[59] R. D. Brown, P. D. Godfrey, D. McNaughton, and A. Pierlot, J. Am. Chem. Soc. **111**, 2308 (1989).
[60] B. Kohler, J. Phys. Chem. Lett. **1**(13), 2047 (2010).
[61] J. Cadet and P. Vigny, in *Bioorganic Photochemistry*, Vol. 1, edited by H. Morrison (Wiley, New York, NY, 1990), pp. 1–272.
[62] C. T. Middleton, B. Cohen, and B. Kohler, J. Phys. Chem. A **111**(42), 10460 (2007).
[63] C. T. Middleton, K. de La Harpe, C. Su, Y. K. Law, C. E. Crespo-Hernández, and B. Kohler, Annu. Rev. Phys. Chem. **60**, 217 (2009).
[64] G. Meijer, G. Berden, W. L. Meerts, H. E. Hunziker, M. S. de Vries, and H. R. Wendt, Chem. Phys. **163**, 209 (1992).
[65] G. Meijer, M. S. de Vries, H. E. Hunziker, and H. R. Wendt, Applied Physics B-Photophysics and Laser Chemistry **51**(6), 395 (1990).
[66] A. Svendsen, U. J. Lorenz, O. V. Boyarkin, and T. R. Rizzo, Rev. Sci. Instrum. **81**(7) (2010).
[67] W. J. Schreier, T. E. Schrader, F. O. Koller, P. Gilch, C. E. Crespo-Hernandez, V. N. Swaminathan, T. Carell, W. Zinth, and B. Kohler, Science **315**(5812), 625 (2007).
[68] A. M. Rijs, M. Kabelac, A. Abo-Riziq, P. Hobza, and M. S. de Vries, ChemPhysChem **12** (10), 1816 (2011).
[69] L. Gonzalez, D. Escudero, and L. Serrano-Andres, Chem. Phys. Chem **13**(1), 28–51 (2012).
[70] E. Plasser, M. Barbatti, A. J. A. Aquino, and H. Lischka, Theor. Chem. Acc. **131**(1) (2012).
[71] O. Christiansen, H. Koch, and P. Jorgensen, Chem. Phys. Lett. **243**, 409 (1995).
[72] A. B. Trofimov and J. Schirmer, J Phys B-at Mol Opt **28**(12), 2299 (1995).
[73] J. Schirmer, Phys. Rev. A **26**(5), 2395 (1982).
[74] C. Hattig and F. Weigend, J. Chem. Phys. **113**(13), 5154 (2000).
[75] A. Kohn and C. Hattig, J. Chem. Phys. **119**(10), 5021 (2003).
[76] R. Bauernschmitt and R. Ahlrichs, Chem. Phys. Lett. **256**(4–5), 454 (1996).
[77] F. Furche and R. Ahlrichs, J. Chem. Phys. **117**(16), 7433 (2002).
[78] E. Tapavicza, I. Tavernelli, and U. Rothlisberger, Phys. Rev. Lett. **98**(2) (2007).
[79] U. Werner, R. Mitric, T. Suzuki, and V. Bonacic-Koutecky, Chem. Phys. **349**(1–3), 319 (2008).
[80] I. Tavernelli, B. F. E. Curchod, and U. Rothlisberger, J. Chem. Phys. **131**(19), 196101 (2009).
[81] R. Send and F. Furche, J. Chem. Phys. **132**(4), 044107 (2010).
[82] M. Barbatti, J. Pittner, M. Pederzoli, U. Werner, R. Mitric, V. Bonacic-Koutecky, and H. Lischka, Chem. Phys. **375**(1), 26 (2010).
[83] R. Shepard. *The Multiconfiguration Self-Consistent Field Method* (Wiley, New York, 1987).

[84] H. Lischka, R. Shepard, F. B. Brown, and I. Shavitt, Int. J. Quantum Chem. **S15**, 91 (1981).
[85] H. Lischka, R. Shepard, R. M. Pitzer, I. Shavitt, M. Dallos, T. Muller, P. G. Szalay, M. Seth, G. S. Kedziora, S. Yabushita, and Z. Y. Zhang, PCCP **3**(5), 664 (2001).
[86] J. Finley, P. A. Malmqvist, B. O. Roos, and L. SerranoAndres, Chem. Phys. Lett. **288**, 299 (1998).
[87] B. H. Lengsfield, P. Saxe, and D. R. Yarkony, J. Chem. Phys. **81**(10), 4549 (1984).
[88] H. Lischka, M. Dallos, and R. Shepard, Mol. Phys. **100**(11), 1647 (2002).
[89] P. Celani and H. J. Werner, J. Chem. Phys. **119**(10), 5044 (2003).
[90] H. Lischka, M. Dallos, P. G. Szalay, D. R. Yarkony, and R. Shepard, J. Chem. Phys. **120**(16), 7322 (2004).
[91] M. R. Silva-Junior and W. Thiel, J. Chem. Theory Comput. **6**(5), 1546 (2010).
[92] H. R. Hudock, B. G. Levine, A. L. Thompson, H. Satzger, D. Townsend, N. Gador, S. Ullrich, A. Stolow, and T. J. Martinez, J. Phys. Chem. A **111**(34), 8500 (2007).
[93] H. R. Hudock and T. J. Martinez, Chem. Phys. Chem. **9**(17), 2486 (2008).
[94] M. Barbatti and H. Lischka, J. Am. Chem. Soc. **130**, 6831 (2008).
[95] M. Barbatti, A. J. A. Aquino, J. J. Szymczak, D. Nachtigallová, P. Hobza, and H. Lischka, Proc. Nat. Acad. Sci. U.S.A. **107**(50), 21453 (2010).
[96] Z. G. Lan, E. Fabiano, and W. Thiel, Chem. Phys. Chem. **10**(8), 1225 (2009).
[97] Z. G. Lan, E. Fabiano, and W. Thiel, J. Phys. Chem. B **113**(11), 3548 (2009).
[98] E. Fabiano and W. Thiel, J. Phys. Chem. A **112**(30), 6859 (2008).
[99] Y. B. Lei, S. A. Yuan, Y. S. Dou, Y. B. Wang, and Z. Y. Wen, J. Phys. Chem. A **112**(37), 8497 (2008).
[100] A. N. Alexandrova, J. C. Tully, and G. Granucci, J. Phys. Chem. B **114**(37), 12116 (2010).
[101] H. Langer, N. L. Doltsinis, and D. Marx, Chem. Phys. Chem. **6**(9), 1734 (2005).
[102] R. Improta, V. Barone, A. Lami, and F. Santoro, J. Phys. Chem. B **113**(43), 14491 (2009).
[103] G. Zechmann and M. Barbatti, J. Phys. Chem. A **112**(36), 8273–9 (2008).
[104] E. Nir, C. Janzen, P. Imhof, K. Kleinermanns, and M. S. de Vries, J. Chem. Phys. **115**, 4604 (2001).
[105] W. Chin, M. Mons, I. Dimicoli, F. Piuzzi, B. Tardivel, and M. Elhanine, European Physical Journal D **20**(3), 347 (2002).
[106] M. Mons, I. Dimicoli, F. Piuzzi, B. Tardivel, and M. Elhanine, J. Phys. Chem. A **106**(20), 5088 (2002).
[107] V. Karunakaran, K. Kleinermanns, R. Improta, and S. A. Kovalenko, J. Am. Chem. Soc. **131** (16), 5839 (2009).
[108] H. Chen and S. H. Li, J. Chem. Phys. **124**, 15 (2006).
[109] F. A. Miannay, T. Gustavsson, A. Banyasz, and D. Markovitsi, J. Phys. Chem. A **114**(9), 3256 (2010).
[110] G. Kampf, L. E. Kapinos, R. Griesser, B. Lippert, and H. Sigel, J. Chem. Soc. Perk. **2**(7), 1320 (2002).
[111] T. Fujiwara, Y. Kamoshida, R. Morita, and M. Yamashita, J. Photochem. and Photobiol. B: Biology **41**, 114 (1997).
[112] J. B. Nielsen, J. Thøgersen, S. K. Jensen, S. B. Nielsen, and S. R. Keiding, PCCP **13**(30), 13821 (2011).
[113] S. Yamazaki, W. Domcke, and A. L. Sobolewski, J. Phys. Chem. A **112**(47), 11965 (2008).
[114] M. Barbatti, J. J. Szymczak, A. J. A Aquino, D. Nachtigallová, and H. Lischka, J. Chem. Phys. **134**, 014304 (2011).
[115] S. Perun, A. L. Sobolewski, and W. Domcke, Chem. Phys. **313**(1–3), 107 (2005).
[116] A. Abo-Riziq, B. O. Crews, I. Compagnon, J. Oomens, G. Meijer, G. Von Helden, M. Kabelac, P. Hobza, and M. S. de Vries, J. Phys. Chem. A **111**(31), 7529 (2007).
[117] E. Nir, I. Hünig, K. Kleinermanns, and M. S. de Vries, Chem. Phys. Chem. **5**(1), 131 (2004).

[118] E. Nir, P. Imhof, K. Kleinermanns, and M. S. de Vries, J. Am. Chem. Soc. **122**(33), 8091 (2000).
[119] D. C. Luhrs, J. Viallon, and I. Fischer, PCCP **3**, 1827 (2001).
[120] E. Nir, K. Kleinermanns, L. Grace, and M. S. de Vries, J. Phys. Chem. A **105**(21), 5106 (2001).
[121] M. G. D. Nix, A. L. Devine, B. Cronin, R. N. Dixon, and M. N. R. Ashfold, J. Chem. Phys. **125**, 13 (2006).
[122] M. N. R. Ashfold, G. A. King, D. Murdock, M. G. D. Nix, T. A. A. Oliver, and A. G. Sage, PCCP **12**(6), 1218 (2010).
[123] N. L. Evans and S. Ullrich, J. Phys. Chem. A **114**(42), 11225–1 (2010).
[124] S. Ullrich, T. Schultz, M. Z. Zgierski, and A. Stolow, J. Am. Chem. Soc. **126**(8), 2262 (2004).
[125] E. Samoylova, H. Lippert, S. Ullrich, I. V. Hertel, W. Radloff, and T. Schultz, J. Am. Chem. Soc. **127**(6), 1782 (2005).
[126] H. H. Ritze, H. Lippert, E. Samoylova, V. R. Smith, I. V. Hertel, W. Radloff, and T. Schultz, J. Chem. Phys. **122**, 22 (2005).
[127] H. Satzger, D. Townsend, M. Z. Zgierski, S. Patchkovskii, S. Ullrich, and A. Stolow, Proc. Nat. Acad. Sci. U.S.A. **103**(27), 10196 (2006).
[128] C. Canuel, M. Elhanine, M. Mons, F. Piuzzi, B. Tardivel, and I. Dimicoli, PCCP **8**(34), 3978 (2006).
[129] C. Z. Bisgaard, H. Satzger, S. Ullrich, and A. Stolow, Chem. Phys. Chem. **10**(1), 101 (2009).
[130] S. A. Oladepo and G. R. Loppnow, J. Phys. Chem. B **115**(19), 6149 (2011).
[131] J. C. A. Boeyens, J. Chem. Crystallogr. **8**, 317 (1978).
[132] L. Blancafort, B. Cohen, P. M. Hare, B. Kohler, and M. A. Robb, J. Phys. Chem. A **109**(20), 4431 (2005).
[133] H. Chen and S. H. Li, J. Phys. Chem. A **109**(38), 8443 (2005).
[134] S. Perun, A. L. Sobolewski, and W. Domcke, J. Am. Chem. Soc. **127**(17), 6257 (2005).
[135] M. Barbatti and H. Lischka, J. Am. Chem. Soc. **130**(21), 6831 (2008).
[136] A. L. Sobolewski, W. Domcke, C. Dedonder-Lardeux, and C. Jouvet, PCCP **4**(7), 1093 (2002).
[137] A. L. Sobolewski and W. Domcke, European Physical Journal D **20**(3), 369 (2002).
[138] L. Blancafort, J. Am. Chem. Soc. **128**, 210 (2006).
[139] H. Chen and S. Lis, J. Phys. Chem. A **109**, 8443 (2005).
[140] C. M. Marian, J. Chem. Phys. **122**, 104314 (2005).
[141] S. B. Nielsen and T. I. Solling, Chem. Phys. Chem **6**(7), 1276 (2005).
[142] S. Perun, A. L. Sobolewski, and W. Domcke, Chem. Phys. **313**, 107 (2005).
[143] W. C. Chung, Z. G. Lan, Y. Ohtsuki, N. Shimakura, W. Domcke, and Y. Fujimura, Phys. Chem. Chem. Phys. **9**(17), 2075 (2007).
[144] M. Barbatti, H. Koppel, R. Shepard, and P. G. Szalay, Chem. Phys. **349**(1–3), Vii (2008).
[145] S. Matsika, J. Phys. Chem. A **109**(33), 7538 (2005).
[146] V. Ludwig, Z. M. da Costa, M. S. Do Amaral, A. C. Borin, S. Canuto, and L. Serrano-Andres, Chem. Phys. Lett. **492**(1–3), 164 (2010).
[147] T. Gustavsson, A. Sharonov, D. Onidas, and D. Markovitsi, Chem. Phys. Lett. **356**(1–2), 49 (2002).
[148] B. Cohen, P. M. Hare, and B. Kohler, J. Am. Chem. Soc. **125**(44), 13594 (2003).
[149] W. J. Schreier, J. Kubon, N. Regner, K. Haiser, T. E. Schrader, W. Zinth, P. Clivio, and P. Gilch, J. Am. Chem. Soc. **131**(14), 5038-+ (2009).
[150] S. Marguet and D. Markovitsi, J. Am. Chem. Soc. **127**(16), 5780 (2005).
[151] S. Mouret, C. Philippe, J. Gracia-Chantegrel, A. Banyasz, S. Karpati, D. Markovitsi, and T. Douki, Org. Biomol. Chem. **8**(7), 1706 (2010).
[152] M. Mantione and B. Pullman, Biochim. Biophys. Acta **91**(3), 387 (1964).

[153] R. O. Rahn and M. N. Patrick, in *Biology*, edtied by S.Y. Wang (Academic Press, New York, NY, 1976), Vol. II, pp. 97–145.)
[154] C. F. Yang, Y. Q. Yu, K. H. Liu, D. Song, L. D. Wu, and H. M. Su, J. Phys. Chem. A **115** (21), 5335 (2011).
[155] T. Climent, I. Gonzalez-Ramirez, R. Gonzalez-Luque, M. Merchan, and L. Serrano-Andres, J. Phys. Chem. Lett. **1**(14), 2072 (2010).
[156] M. C. Cuquerella, V. Lhiaubet-Vallet, F. Bosca, and M. A. Miranda, Chem. Sci. **2**(7), 1219 (2011).
[157] D. N. Nikogosyan and V. S. Letokhov, Riv Nuovo Cimento **6**(8), 1 (1983).
[158] M. Gueron, J. Eisinger and A. A. Lamola, in *Basic Principles in Nucleic Acid Chemistry*, edited by Ts'o POP (Academic Press, New York, NY, 1974), pp. 311–398.
[159] C. Salet and R. Bensasson, Photochem. Photobiol. **22**(6), 231 (1975).
[160] C. Salet, R. Bensasson, and R. S. Becker, Photochem. Photobiol. **30**(3), 325 (1979).
[161] P. D. Wood and R. W. Redmond, J. Am. Chem. Soc. **118**(18), 4256 (1996).
[162] B. B. Brady, L. A. Peteanu, and D. H. Levy, Chem. Phys. Lett. **147**, 538 (1988).
[163] M. R. Viant, R. S. Fellers, R. P. Mclaughlin, and R. J. Saykally, J. Chem. Phys. **103**(21), 9502 (1995).
[164] R. D. Brown, P. D. Godfrey, D. McNaughton, and A. Pierlot, J. Am. Chem. Soc. **110**, 2329 (1988).
[165] M. Kunitski, Y. Nosenko, and B. Brutschy, Chem. Phys. Chem. **12**(10), 2024 (2011).
[166] Y. G. He, C. Y. Wu, and W. Kong, J. Phys. Chem. A **108**(6), 943 (2004).
[167] M. Busker, M. Nispel, T. Häber, K. Kleinermanns, M. Etinski, and T. Fleig, Chem. Phys. Chem. **9**(11), 1570 (2008).
[168] M. Etinski, T. Fleig, and C. Marian, J. Phys. Chem. A **113**(43), 11809 (2009).
[169] M. A. Elsayed, J. Chem. Phys. **38**(12), 2834 (1963).
[170] C. M. Marian, F. Schneider, M. Kleinschmidt, and J. Tatchen, European Physical Journal D **20** (3), 357 (2002).
[171] P. M. Hare, C. T. Middleton, K. I. Mertel, J. M. Herbert, and B. Kohler, Chem. Phys. **347**(1–3), 383 (2008).
[172] J. J. Szymczak, M. Barbatti, J. T. S. Hoo, J. A. Adkins, T. L. Windus, D. Nachtigallová, and H. Lischka, J. Phys. Chem. A **113**(45), 12686 (2009).
[173] S. Perun, A. L. Sobolewski, and W. Domcke, J. Phys. Chem. A **110**, 13238 (2006).
[174] S. Matsika, J. Phys. Chem. A **108**, 7584 (2004).
[175] D. Nachtigallová, A. J. A. Aquino, J. J. Szymczak, M. Barbatti, P. Hobza, and H. Lischka, J. Phys. Chem. A **115**(21), 5247 (2011).
[176] Y. Mercier, F. Santoro, M. Reguero, and R. Improta, J. Phys. Chem. B **112**(35), 10769 (2008).
[177] G. Medoff and M. N. Swartz, J. Gen. Virol. **4**, 15 (1969).
[178] T. H. Milhorat, P. A. Bolognese, M. Nishikawa, C. A. Francomano, N. B. McDonnell, C. Roonprapunt, and R. W. Kula, Surg Neurol.(Copyright (C) 2011 U.S. National Library of Medicine.) **72**, 20 (2009).
[179] T. H. Milhorat, P. A. Bolognese, M. Nishikawa, C. A. Francomano, N. B. McDonnell, C. Roonprapunt, and R. W. Kula, Surg Neurol.(Copyright (C) 2011 U.S. National Library of Medicine.) **7**, 601 (2007).
[180] A. T. Krueger and E. T. Kool, Curr. Opin. Chem. Biol. **11**(6), 588 (2007).
[181] M. Barbatti, A. J. A. Aquino, J. J. Szymczak, D. Nachtigallová, and H. Lischka, PCCP **13** (13), 6145 (2011).
[182] N. Ismail, L. Blancafort, M. Olivucci, B. Kohler, and M. A. Robb, J. Am. Chem. Soc. **124** (24), 6818 (2002).
[183] A. L. Sobolewski and W. Domcke, PCCP **6**, 2763 (2004).
[184] M. Z. Zgierski, T. Fujiwara, and E. C. Lim, Chem. Phys. Lett. **463**(4–6), 289 (2008).

[185] M. Z. Zgierski, S. Patchkovskii, and E. C. Lim, J. Chem. Phys. **123**(8), 081101 (2005).
[186] J. Gonzalez-Vazquez and L. Gonzalez, ChemPhysChem **11**(17), 3617 (2010).
[187] C. E. Crespo-Hernandez, B. Cohen, and B. Kohler, Nature **436**(7054), 1141 (2005).
[188] T. Takaya, C. Su, K. de La Harpe, C. E. Crespo-Hernandez, and B. Kohler, Proc. Nat. Acad. Sci. U.S.A. **105**(30), 10285 (2008).
[189] C. E. Crespo-Hernández, K. de La Harpe, and B. Kohler, J. Am. Chem. Soc. **130**, 10844 (2008).
[190] C. E. Crespo-Hernandez and B. Kohler, J. Phys. Chem. B **108**(30), 11182 (2004).
[191] N. J. Kim, J. Chang, H. M. Kim, H. Kang, T. K. Ahn, J. Heo, and S. K. Kim, Chem. Phys. Chem. **12**(10), 1935 (2011).
[192] P. Hobza and J. Sponer, J. Am. Chem. Soc. **124**(39), 11802 (2002).
[193] H. Saigusa, S. Urashima, H. Asami, and M. Ohba, J. Phys. Chem. A **114**(42), 11231 (2010).
[194] A. Abo-Riziq, B. Crews, L. Grace, and M. S. de Vries, J. Am. Chem. Soc. **127**(8), 2374 (2005).
[195] F. Piuzzi, M. Mons, I. Dimicoli, B. Tardivel, and Q. Zhao, Chem. Phys. **270**(1), 205 (2001).
[196] M. P. Callahan, Z. Gengeliczki, N. Svadlenak, H. Valdes, P. Hobza, and M. S. de Vries, PCCP **10**(19), 2819 (2008).
[197] A. Abo-Riziq, L. Grace, E. Nir, M. Kabelac, P. Hobza, and M. S. de Vries, Proc. Nat. Acad. Sci. U.S.A. **102**(1), 20 (2005).
[198] A. L. Sobolewski, W. Domcke, and C. Hättig, PNAS **102**, 17903 (2005).
[199] S. Perun, A. L. Sobolewski, and W. Domcke, J. Phys. Chem. A **110**(29), 9031 (2006).
[200] J. Catalan, F. Fabero, R. M. Claramunt, M. D. S. Maria, M. D. C. Focesfoces, F. H. Cano, M. Martinezripoll, J. Elguero, and R. Sastre, J. Am. Chem. Soc. **114**(13), 5039 (1992).
[201] E. Nir, C. Janzen, P. Imhof, K. Kleinermanns, and M. S. de Vries, PCCP **4**(5), 740 (2002).
[202] E. Nir, C. Janzen, P. Imhof, K. Kleinermanns, and M. S. de Vries, PCCP **4**(5), 732 (2002).
[203] L. Biemann, S. A. Kovalenko, K. Kleinermanns, R. Mahrwald, M. Markert, and R. Improta, J. Am. Chem. Soc. **133**(49), 19664 (2011).
[204] T. Schultz, E. Samoylova, W. Radloff, I. V. Hertel, A. L. Sobolewski, and W. Domcke, Science **306**(5702), 1765 (2004).
[205] E. Nir, C. Plützer, K. Kleinermanns, and M. de Vries, European Physical Journal D **20**(3), 317 (2002).
[206] S. Yamazaki and T. Taketsugu, PCCP **14**(25), 8866 (2012).
[207] N. K. Schwalb, T. Michalak, and F. Temps, J. Phys. Chem. B **113**(51), 16365 (2009).
[208] N. K. Schwalb and F. Temps, J. Am. Chem. Soc. **129**(30), 9272-+ (2007).
[209] K. de La Harpe, C. E. Crespo-Hernandez, and B. Kohler, Chem. Phys. Chem **10**(9–10), 1421 (2009).
[210] K. de La Harpe, C. E. Crespo-Hernandez, and B. Kohler, J. Am. Chem. Soc. **131**(48), 17557 (2009).
[211] K. Kobayashi and S. Tagawa, J. Am. Chem. Soc. **125**(34), 10213 (2003).
[212] K. Hunger, L. Buschhaus, L. Biemann, M. Braun, S. A. Kovalenko, R. Improta and K. Kleinermanns, Chem. Eur. J. (in press).
[213] T. Giorgi, F. Grepioni, I. Manet, P. Mariani, S. Masiero, E. Mezzina, S. Pieraccini, L. Saturni, G. P. Spada, and G. Gottarelli, Chem-Eur J **8**(9), 2143 (2002).
[214] C. Plützer, I. Hünig, K. Kleinermanns, E. Nir, and M. S. de Vries, Chem. Phys. Chem. **4**(8), 838 (2003).
[215] M. Dargiewicz, M. Biczysko, R. Improta, and V. Barone, PCCP **14**(25), 8981 (2012).
[216] C. Plützer, I. Hünig, and K. Kleinermanns, PCCP **5**(6), 1158 (2003).
[217] A. T. Krueger and E. T. Kool, Chem. Biol. **16**(3), 242 (2009).
[218] C. R. Geyer, T. R. Battersby, and S. A. Benner, Structure **11**(12), 1485 (2003).
[219] S. Miyakawa, H. J. Cleaves, and S. L. Miller, Origins Life Evol. Biosphere **32**(3), 209 (2002).

[220] Z. Gengeliczki, M. P. Callahan, M. Kabelac, A. M. Rijs, and M. S. de Vries, J. Phys. Chem. A **115**(41), 11423 (2011).
[221] B. O. Crews, A. Abo-Riziq, K. Pluhackova, P. Thompson, G. Hill, P. Hobza, and M. S. de Vries, PCCP **12**(14), 3597 (2010).
[222] I. Vaya, F. A. Miannay, T. Gustavsson, and D. Markovitsi, Chem. Phys. Chem. **11**(5), 987 (2010).
[223] I. Vaya, P. Changenet-Barret, T. Gustavsson, D. Zikich, A. B. Kotlyar, and D. Markovitsi, Photoch. Photobio. Sci. **9**(9), 1193 (2010).
[224] D. Markovitsi, T. Gustavsson, and A. Banyasz, Mutat Res-Rev Mutat **704**(1–3), 21 (2010).
[225] Y. K. Law, J. Azadi, C. E. Crespo-Hernandez, E. Olmon, and B. Kohler, Biophys. J. **94**(9), 3590 (2008).
[226] S. Rössle, J. Friedrichs, and I. Frank, Chem. Phys. Chem. **11**(9), 2011 (2010).
[227] M. Hariharan, M. McCullagh, G. C. Schatz, and F. D. Lewis, J. Am. Chem. Soc. **132**(37), 12856 (2010).
[228] W. J. Schreier, J. Kubon, P. Clivio, W. Zinth, and P. Gilch, Spectrosc-Int J **24**(3–4), 309 (2010).
[229] S. Asgatay, A. Martinez, S. Coantic-Castex, D. Harakat, C. Philippe, T. Douki, and P. Clivio, J. Am. Chem. Soc. **132**(30), 10260 (2010).
[230] D. Roca-Sanjuan, G. Olaso-Gonzalez, I. Gonzalez-Ramirez, L. Serrano-Andres, and M. Merchan, J. Am. Chem. Soc. **130**(32), 10768 (2008).
[231] M. Boggio-Pasqua, G. Groenhof, L. V. Schafer, H. Grubmuller, and M. A. Robb, J. Am. Chem. Soc. **129**, 10996 (2007).
[232] L. Lapinski, H. Rostkowska, A. Khvorostov, R. Fausto, and M. J. Nowak, J. Phys. Chem. A **107**(31), 5913 (2003).
[233] L. Buschhaus, J. Rolf and K. Kleinermanns, *A New Photo Degradation Pathway of DNA: Norrish I Alpha-cleavage to Labile Isocyanates* (forthcoming).
[234] I. Reva, M. J. Nowak, L. Lapinski, and R. Fausto, J. Phys. Chem. B **116**(19), 5703 (2012).
[235] C. E. Crespo-Hernandez and B. Kohler, J. Phys. Chem. B **108**, 11182 (2004).
[236] D. Markovitsi, T. Gustavsson, and F. Talbot, Photochem. Photobiol. Sci. **6**, 717 (2007).
[237] F. -A. Miannay, Á. Bányász, T. Gustavsson, and D. Markovitsi, J. Am. Chem. Soc. **129**, 14574 (2007).
[238] D. Onidas, T. Gustavsson, E. Lazzarotto, and D. Markovitsi, J. Phys. Chem. B **111**, 9644 (2007).
[239] B. Bouvier, J. P. Dognon, R. Lavery, D. Markovitsi, P. Millie, D. Onidas, and K. Zakrzewska, J. Phys. Chem. B **107**(48), 13512 (2003).
[240] A. I. Kononov, V. M. Bakulev, and V. L. Rapoport, J. Photochem. Photobiol. B: Biol. **19**, 139 (1993).
[241] R. Plessow, A. Brockhinke, W. Eimer, and Kohse-Hoinghaus, J. Phys. Chem. B **104**, 3695 (2000).
[242] I. Buchvarov, Q. Wang, M. Raytchev, A. Trifonov, and T. Fiebig, Proc. Nat. Acad. Sci. U.S. A. **104**(12), 4794 (2007).
[243] D. Markovitsi, F. Talbot, T. Gustavsson, D. Onidas, E. Lazzarotto, and S. Marguet, Nature **441**(7094), E7 (2006).
[244] D. Markovitsi, A. Sharonov, D. Onidas, and T. Gustavsson, Chem. Phys. Chem. **4**(3), 303 (2003).
[245] T. Gustavsson, R. Improta, and D. Markovitsi, J. Phys. Chem. Lett. **1**(13), 2025 (2010).
[246] B. Bouvier, T. Gustavsson, D. Markovitsi, and P. Millie, Chem. Phys. **275**(1–3), 75 (2002).
[247] E. Emanuele, D. Markovitsi, P. Millie, and K. Zakrzewska, ChemPhysChem **6**(7), 1387 (2005).
[248] H. H. Ritze, P. Hobza, and D. Nachtigallová, Phys. Chem. Chem. Phys. **9**, 1672 (2007).
[249] D. Nachtigallová, P. Hobza, and H. H. Ritze, PCCP **10**(37), 5689 (2008).

[250] F. Santoro, V. Barone, and R. Improta, J. Comput. Chem. **29**(6), 957 (2008).
[251] F. Santoro, V. Barone, and R. Improta, Chem. Phys. Chem. **9**(17), 2531 (2008).
[252] F. Santoro, V. Barone, and R. Improta, J. Am. Chem. Soc. **131**(42), 15232 (2009).
[253] E. B. Starikov, G. Cuniberti, and S. Tanaka, J. Phys. Chem. B **113**(30), 10428 (2009).
[254] F. Santoro, V. Barone, A. Lami, and R. Improta, PCCP **12**(19), 4934 (2010).
[255] E. R. Bittner, J Photoch Photobio A **190**(2–3), 328 (2007).
[256] Czader and E. R. Bittner, J. Chem. Phys. **128**(3), 035101 (2008).
[257] D. Nachtigallová, T. Zeleny, M. Ruckenbauer, T. Muller, M. Barbatti, P. Hobza, and H. Lischka, J. Am. Chem. Soc. **132**, 8261 (2010).
[258] T. Zeleny, P. Hobza, D. Nachtigallová, M. Ruckenbauer, and H. Lischka, Collect. Czech. Chem. Commun. **76**, 631 (2011).
[259] I. Conti, P. Altoe, M. Stenta, M. Garavelli, and G. Orlandi, PCCP **12**(19), 5016 (2010).
[260] Z. G. Lan, Y. Lu, E. Fabiano, and W. Thiel, ChemPhysChem **12**(10), 1989 (2011).
[261] Y. Lu, Z. G. Lan, and W. Thiel, Angew. Chem. Int. Ed. **50**(30), 6864 (2011).
[262] F. Santoro, V. Barone, and R. Improta, Proc. Nat. Acad. Sci. U.S.A. **104**(24), 9931 (2007).
[263] G. Olaso-Gonzáles, D. Roca-Sanjuán, L. Serrano-Andres, and M. Merchan, J. Chem. Phys. A **125**, 231102 (2006).
[264] L. H. Hu, Y. Zhao, F. Wang, G. H. Chen, C. S. Ma, W. M. Kwok, and D. L. Phillips, J. Phys. Chem. B **111**(40), 11812 (2007).
[265] R. Improta, PCCP **10**(19), 2656 (2008).
[266] O. V. Boyarkin, S. R. Mercier, A. Kamariotis, and T. R. Rizzo, J. Am. Chem. Soc. **128**(9), 2816 (2006).